



# **Superomniphobic Surfaces for Military Applications: Nano- and Micro-Fabrication Methods**

## *Chapter 2: Investigation of Wear for Superhydrophobic Surfaces and Development of New Coatings*

*Alidad Amirfazli  
University of Alberta*

*University of Alberta  
Department of Mechanical Engineering  
Edmonton, AB T6G 2G8*

*PWGSC Contract Number: W7707-098197  
Contract Scientific Authority: Paul Saville, 250-363-2892*

*The scientific or technical validity of this Contract Report is entirely the responsibility of the contractor and the contents do not necessarily have the approval or endorsement of Defence R&D Canada.*

## **Defence R&D Canada – Atlantic**

Contract Report  
DRDC Atlantic CR 2010-315  
January 2011

This page intentionally left blank.

# **Superomniphobic Surfaces for Military Applications: Nano- and Micro-Fabrication Methods**

*Chapter 2: Investigation of Wear for Superhydrophobic Surfaces and Development of New Coatings*

Alidad Amirfazli  
University of Alberta

University of Alberta  
Department of Mechanical Engineering  
Edmonton, Alberta T6G 2G8

PWGSC Contract Number: W7707-098197  
CSA: Paul Saville, 250-363-2892

The scientific or technical validity of this Contract Report is entirely the responsibility of the Contractor and the contents do not necessarily have the approval or endorsement of Defence R&D Canada.

**Defence R&D Canada – Atlantic**

Contract Report  
DRDC Atlantic CR 2010-315  
January 2011

Principal Author

*Original signed by Alidad Amirfazli*

---

Alidad Amirfazli

Approved by

*Original signed by Terry Foster*

---

Terry Foster

Head Dockyard Laboratory Pacific

Approved for release by

*Original signed by Ron Kuwahara for*

---

Calvin Hyatt

Head Document Review Panel

This Work Sponsored by 12S through 12SZ20

© Her Majesty the Queen in Right of Canada, as represented by the Minister of National Defence, 2011

© Sa Majesté la Reine (en droit du Canada), telle que représentée par le ministre de la Défense nationale, 2011

## Abstract

---

The results of wearing superhydrophobic surfaces and its effect on roughness parameters, surface properties and wetting behaviour are described in this report. An abrasive wear device has been set up to allow consistency, reproducibility and precise control over the amount of wear desired. Based on the results obtained, relationships in the trends observed with the different roughness parameters and wetting behaviour have been established. In some cases the relationships are strong while in other cases, the relationships are weak and unable to capture the different transitions in wetting. It has also been determined that different roughness scales present on a surface wear differently and require separate attention. This knowledge is partly applied in the development of a versatile superhydrophobic coating that can be used on smooth and rough materials ranging from glass and aluminum, to polyester/nylon, cardboard and wood.

## Résumé

---

Le présent rapport contient la description de l'usure subie par des surfaces superhydrophobes et de ses effets sur les paramètres de rugosité, les propriétés de surface et le comportement au mouillage. On a mis en place un dispositif d'usure par abrasion qui permet d'assurer un contrôle précis, uniforme et reproductible du degré d'usure souhaité. Les résultats obtenus ont permis d'établir des relations à partir des tendances observées pour les différents paramètres de rugosité et le comportement au mouillage. Dans certains cas, les relations sont solides ( $R_{sk}$ ,  $S_{sk}$ ,  $r$ ), alors que dans d'autres, elles sont faibles ( $R_a$ ,  $R_q$ ,  $R_z$ ) et ne permettent pas d'extraire les diverses transitions qui surviennent au cours du mouillage. Les résultats ont aussi permis de déterminer que des zones de la surface caractérisées par diverses échelles de rugosité subissent une usure différente et nécessitent donc des mesures de protection distinctes. Ces connaissances peuvent être en partie utilisées pour mettre au point un revêtement superhydrophobe polyvalent pouvant être appliqué sur des matériaux lisses et rugueux, dans une gamme allant du verre et de l'aluminium au carton et au bois, en passant par des polymères comme les polyesters et les nylons.

This page intentionally left blank.

## Executive summary

---

### **Superomniphobic Surfaces for Military Applications: Nano- and Micro-Fabrication Methods: Chapter 2: Investigation of Wear for Superhydrophobic Surfaces and Development of New Coatings**

**Alidad Amirfazli; DRDC Atlantic CR 2010-315; Defence R&D Canada – Atlantic; January 2011**

**Introduction:** The properties of superhydrophobic materials are dependent on the surface roughness and surface energy. Experimental materials typically suffer from wear which results in a loss of the superhydrophobic properties. In order to understand the impact of wear on the roughness and hence the desired properties, surface roughness parameters are characterized by confocal scanning microscopy and then materials are subjected to wear.

**Results:** Superhydrophobic PTFE, and acid etched aluminum were used to study wear. A wear test was developed. Certain roughness parameters were found to be strongly correlated to transitions in the wettability of the surface. It was also noted that wear was not uniform across all roughness scales. These studies were partly used to develop a new multipurpose superhydrophobic material.

**Significance:** The success of a superhydrophobic or superorganophobic material will depend on its durability. Loss of roughness will reduce a material's ability to shed liquids. Test methods that accurately predict change in a surface's properties are required for quantifying material durability.

**Future plans:** With the development of a reproducible multipurpose superhydrophobic coating, it is now possible to correlate surface roughness parameters and wettability more thoroughly. The newly developed coating has so far been used to demonstrate its suitability for use on a variety of surfaces and still requires further testing.

## Sommaire

---

### **Superomniphobic Surfaces for Military Applications: Nano- and Micro-Fabrication Methods: Chapter 2: Investigation of Wear for Superhydrophobic Surfaces and Development of New Coatings**

**Alidad Amirfazli; DRDC Atlantic CR 2010-315; R & D pour la défense Canada – Atlantique; Janvier 2011**

**Introduction :** Les propriétés des matériaux superhydrophobes dépendent de la rugosité de la surface et de l'énergie superficielle. Les matériaux expérimentaux subissent couramment l'usure qui entraîne une perte de leurs propriétés superhydrophobes. Afin de bien comprendre les effets de l'usure sur la rugosité de la surface et, conséquemment, sur les propriétés souhaitées, on a caractérisé des paramètres de rugosité de la surface en observant des échantillons de matériaux par microscopie confocale à balayage, avant de les soumettre à des essais d'usure.

**Résultats :** Les deux matériaux étudiés dans des essais d'usure élaborés dans nos installations sont du PTFE [poly(tétrafluoroéthylène)] superhydrophobe et de l'aluminium gravé à l'acide. Les résultats des essais indiquent qu'il existe une corrélation élevée entre certains paramètres de rugosité et les étapes de transition au cours du mouillage de la surface. On observe aussi que l'usure n'est pas uniforme pour l'ensemble des échelles de rugosité. Ces connaissances ont été en partie utilisées pour mettre au point un nouveau revêtement superhydrophobe polyvalent.

**Importance :** L'utilisation pratique et adéquate d'un matériau superhydrophobe ou superorganophobe sera fonction de sa durabilité. Une perte de rugosité réduit la capacité d'un matériau de laisser l'eau s'écouler à sa surface. Il est essentiel d'élaborer des méthodes d'essai fiables, qui permettent de prévoir avec exactitude les variations des propriétés de surface, afin de pouvoir quantifier la durabilité d'un matériau.

**Perspectives :** La mise au point d'un revêtement superhydrophobe polyvalent possédant des propriétés reproductibles permet maintenant d'établir des corrélations plus détaillées entre des paramètres de rugosité de la surface et sa mouillabilité. Jusqu'à maintenant, le nouveau revêtement a uniquement servi à démontrer qu'il constitue un produit d'induction adéquat pour toute une gamme de surfaces; c'est pourquoi il faudra réaliser des essais plus poussés en ce domaine.



# Table of contents

---

Abstract .....	i
Résumé .....	i
Executive summary .....	iii
Sommaire .....	iv
Table of contents .....	v
List of figures .....	vii
List of tables .....	xii
1 Introduction.....	1
2 Wearing Plasma Etched PTFE.....	4
2.1 PHASE I.....	4
2.1.1 Experimental Details.....	4
2.1.1.1 First Part: Experimental Set-up and Feasibility Investigation .....	4
2.1.1.2 Second Part: Preliminary Experiments, Observations and Quantitative Analysis .....	7
2.1.1.3 Third Part: Experimental Work with Complete Quantitative Data Collection and Analysis .....	8
2.2 PHASE II.....	13
2.3 PHASE III .....	17
3 Wearing Aluminum Foil Coated with Superhydrophobic Coating. ....	18
3.1 PROCEDURE .....	18
3.2 EXPERIMENTAL DETAILS.....	19
3.2.1 First Sample - Unworn:.....	19
3.2.2 Second Sample - Worn by stomping from using as mat: .....	20
3.2.3 Third Sample - Worn by stomping from using as mat + 8 minutes on shaker: .....	21
3.3 RESULTS AND ANALYSIS .....	23
3.3.1 SEM Images.....	23
3.3.1.1 First Sample - Unworn: .....	23
3.3.1.2 Second Sample - Worn by stomping from using as mat: .....	25
3.3.1.3 Third Sample - Worn by stomping from using as mat + 8 minutes on shaker: .....	27
3.3.2 CSM Data.....	27
3.4 CONCLUSIONS .....	29
4 Developing Superhydrophobic Coating.....	31
4.1 EXPERIMENTAL DETAILS.....	32
4.1.1 BATCH # 1 .....	32
4.1.2 BATCH # 2 .....	34

4.1.3	BATCH # 3 .....	36
4.2	RESULTS AND ANALYSIS .....	38
5	CONCLUSIONS AND FUTURE WORK .....	42
	References .....	43
	Annex A .. Cleaning Procedure for Samples Worn in Shaker .....	45
	Annex B... Procedure for Wearing Superhydrophobic Samples Abrasively with Shaker .....	47
	Annex C... Drop Weight Wear Testing Procedure .....	51
	List of symbols/abbreviations/acronyms/initialisms .....	53
	Distribution list .....	55

## List of figures

---

Figure 1: SEM Image of unworn Plasma Etched PTFE. The roughness and pillars can be clearly observed. Image scale is 2 $\mu\text{m}$ .....	5
Figure 2: SEM Image of Plasma Etched PTFE sample after being worn with sand. The sample has not been cleaned after wearing and shows the presence of small sand particles roughly 2 $\mu\text{m}$ in size. Image scale is 2 $\mu\text{m}$ .....	6
Figure 3: SEM Image of Plasma Etched PTFE sample after being worn with sand. The sample has been cleaned in an ultrasonic bath after wearing and still shows the presence of small sand particles roughly 2 $\mu\text{m}$ in size. Image scale is 2 $\mu\text{m}$ . ....	6
Figure 4: SEM Image of Plasma Etched PTFE sample after being worn with glass beads. The sample has not been cleaned after wearing and shows the presence of one glass bead roughly 25 $\mu\text{m}$ in diameter. Notice there is no contamination visible on the rest of the image. Image scale is 10 $\mu\text{m}$ . ....	7
Figure 5: SEM Image of unworn Acid Etched superhydrophobic Aluminum shows various levels of roughness. Image scale is 10 $\mu\text{m}$ . ....	8
Figure 6: SEM Image of an Acid Etched superhydrophobic Aluminum sample worn with glass beads for 5 minutes at 300 rpm. Sample has lost most of its roughness and is no longer hydrophobic. Image scale is 10 $\mu\text{m}$ . ....	8
Figure 7: Advancing, Receding and Hysteresis contact angles of water vs. wear time for Plasma Etched PTFE. A decreasing Receding contact angle can be seen as wear time increases. The difference between the Advancing and the Receding contact angles is plotted as the Hysteresis. This difference is observed as pinning of the drop when it is receding. Sample was worn at 200 rpm with 1/2 inch glass bead depth in 30 seconds wear intervals.....	9
Figure 8: A water drop receding across a worn Plasma Etched PTFE sample. The water drop is receding from a) to c). This transition is defined as “pinning” as the points where the drop contacts the surface remain at the same place (constant contact radius) with a decreasing receding contact angle. The white line in the images is a constant length throughout and is just a reference line to show a constant contact radius. <sup>5</sup> .....	10
Figure 9: A plot of contact radius against the contact angle as a water drop is first advancing, then pinning, and then receding across a worn plasma etched PTFE sample. During the pinning transition, the contact radius remains fairly constant while the contact decreases until the water droplet starts receding at a lower contact angle. <sup>5</sup> Sample worn at 200 rpm with 1/2 inch glass bead height at 30 seconds wear intervals. ....	10
Figure 10: Plot of skewness parameters (Rsk left and Ssk right) for Plasma Etched PTFE sample worn at 200 rpm 1/2 inch of glass beads at 30 second intervals. This parameter shows a jump between 3 and 3.5 minutes (with relatively constant values before and after). This is the same sudden change seen for the wetting data in Figure 7. ....	11

Figure 11: Plot of the  $r$  parameter for worn Plasma Etched PTFE sample shows a sharp decrease in rough surface area with increased wear time. .... 12

Figure 12: Plot of the  $S_{ds}$  parameter for worn Plasma Etched PTFE sample shows an increasing trend with wear time and also captures the sudden change in wetting at 3-3.5 minutes..... 12

Figure 13: Contact Angles of water with Wear Time (in minutes). Contact angle on the left axis and hysteresis on the right axis. This figure clearly shows little to no change in hysteresis for a total of 270 seconds (4.5 minutes) of wear time. At 300 seconds (5 minutes), a clear jump in hysteresis is observed marking the beginning of the pinning behaviour shown in Figure 14. Sample was worn at 195 rpm in 1 inch of glass bead depth at 30 seconds intervals. .... 14

Figure 14: Pinning behaviour of water drop in the receding phase of the wetting test. This behaviour is indicative of the surface starting to lose its superhydrophobicity. a) Before pinning with contact radius  $r_0$  and receding at a contact angle  $\theta_0$ . b) Last frame of pinning behaviour with the same contact radius  $r_0$  from 'a' but a lower contact angle  $\theta_1$ . c) Right after releasing from pinning with drop receding at a lower contact radius  $r_1$  than 'a' and 'b' but at the same contact angle  $\theta_0$  as from 'a'. .... 14

Figure 15: Plot of the non-dimensional  $S_{sk}$  parameter (volumetric skewness) vs. Wear Time shows an increasing trend with observed pinning for a Plasma Etched PTFE sample worn at 195 rpm in 1 inch of glass bead depth at 30 seconds wear intervals. .... 15

Figure 16: Plots of the surface area ratio ( $r$  parameter) and the ratio of solid surface area wet ( $f$  parameter) vs. wear time. The plot for  $r$  shows a decreasing trend with increasing wear time reaching its lowest point at 300 seconds (5 minutes) of wear, also the same point at which hysteresis is highest. The plot for  $f$  however, shows a very slight increase in surface area wet by the liquid, yet not a strong enough trend to directly connect to wetting. Plasma Etched PTFE sample worn at 195 rpm in 1 inch of glass bead depth at 30 seconds wear intervals. .... 16

Figure 17: Water drop laying on a flat sample of unworn aluminum foil coated with superhydrophobic coating. a) Side view. b) Angled view. It can be clearly observed that the drop is somewhat spherical in shape (despite its volume) with a circular contact area and high contact angle. Once this surface became slightly tilted, any water drops would immediately roll off. .... 20

Figure 18: Water drop laying on a flat sample of stomped aluminum foil coated with superhydrophobic coating. Sample appears to be as superhydrophobic as the first. Some yellow specks not visible in the first (unworn) sample are circled. a) Side view. b) Angled view c) Top view. .... 21

Figure 19: Water drop on third sample when tilted at a slight angle ( $\sim 10^\circ - 15^\circ$ ) with water roll-off direction noted by the dashed arrow. The drop pins on its trailing edge (left side of drop shown with solid arrow) causing the drop to no longer have a circular contact area and to adopt a teardrop-like shape. Also, small drops (circled areas) do not roll off the surface easily. Pockets of air between the surface roughness and the water drop (Cassie-Baxter model<sup>4</sup> and Figure 20) can also be

seen on the three images (specially on c). On a smooth surface, surface refraction through the drop looks smooth. a) Top view. b) Angled view. c) Close-up of pinning point and air pockets visible through the drop. .... 22

Figure 20: Cassie-Baxter model describes no penetration of the liquid into the surface's roughness (black grooves). The liquid therefore sits on the peaks of the roughness and on the pockets of air (white sections between the black grooves). Drop size and roughness features are not to scale. Usually roughness features are in the order of  $\mu\text{m}$  and  $\text{nm}$  while drops are in the order of  $\text{mm}$  and  $\text{cm}$  (Image and wording used with the kind permission of Parham Zabeti)..... 22

Figure 21: Small water drops stick to the surface of the third sample when tilted vertically ( $90^\circ$ ). This shows that the surface has been worn to some extent since this behaviour is not seen on the first or second sample. The drops stick to the surface because of the changes in the topography of the sample's surface and perhaps also because of the creases created (and visible) from when the sample was stomped on..... 23

Figure 22: SEM Images of the first sample (unworn) at 100X, 500X, 2,500X, 5,000X and 50,000X magnification respectively taken at a tilt of  $45^\circ$  showing the detail and different sizes of the roughness features. This sample was coated with the Organoclay Nanocomposite Superhydrophobic Film from the University of Illinois.<sup>9</sup> No details were provided with this sample regarding coating thickness or coating technique. .... 24

Figure 23: SEM Images of the second sample (worn by stomping from using as mat) at 100X, 500X, 2,500X, 5,000X and 50,000X magnification respectively taken at a tilt of  $45^\circ$  showing the detail and different sizes of the roughness features. This sample was coated with the Organoclay Nanocomposite Superhydrophobic Film from the University of Illinois.<sup>9</sup> No addition details were provided with this sample regarding coating thickness or coating technique. It was only mentioned that this sample had been stomped on and/or used as a mat ..... 26

Figure 24: Sa and Sq parameters are the volumetric counterparts of Ra and Rq and are plotted at three different magnifications (20X, 50X and 100X) for the three samples tested. It can be seen that the values for each magnification follow the same trend. However, the 100X magnification data is shifted. This relates to the idea of having more than one roughness scale and its effects on roughness measurements.<sup>6</sup> ..... 28

Figure 25: Ssk and Sku parameters are the volumetric counterparts of Rsk and Rku and are plotted at three different magnifications (20X, 50X and 100X) for the three samples tested. It can be seen that the trends for each magnification are very different from each other unlike the plots for Sa and Sq in Figure 24. Ssk and Sku parameters seem to converge at the third sample (the most worn sample), yet the different trends also relate to the idea of having more than one roughness scale. .... 28

Figure 26: r parameter plotted at three different magnifications (20X, 50X and 100X) for the three different samples. The trends for each magnification are similar to the trends of Sa and Sq. This parameter shows an increasing trend meaning that more surface area has been developed with wear. For this to be possible, either the coatings between samples are different, or, subjecting the surface to wear has

modified the original roughness in a way that has increased the distance between the peaks and the valleys.....	29
Figure 27: 5,000X SEM Images of one coat of the first batch of superhydrophobic coating without additional Teflon™ coating (scale is 2 μm for the three images). It can be seen that this mix (without Zonyl®) seems to provide the required surface roughness to satisfy the Cassie-Baxter wetting model. However, a significant difference can be observed between the sizes of the roughness features in the three samples, with sample 1 having the roughest appearance. a) Heavy coat on aluminum foil. b) Light coat on copper tape. c) Light coat on aluminum foil.....	33
Figure 28: 1,000X SEM images taken at 45° of the second batch of coating applied in light coats on Sample 1 (scale is 10 μm for the three images). It can be seen that there are portions of aluminum foil that were not covered (areas denoted by white arrows). It can also be observed that the roughness of the coatings is very different with Zonyl® incorporated in the mixture. The roughness features do not look as jagged and sharp as they did in Figure 27. a) 1 Coat. b) 2 Coats. c) 3 Coats.....	34
Figure 29: 1,000X SEM images taken at 45° of the second batch of coating applied in medium coats on Sample 2 (scale is 10 μm for the three images). There are still portions of aluminum foil that were not covered (areas denoted by white arrows) with the first coat. Coating is apparently more even than with the thinner coats from Figure 28. a) 1 Coat. b) 2 Coats. c) 3 Coats. ....	35
Figure 30: 1,000X SEM images taken at 45° of the second batch of coating applied in heavy coats on Sample 3 (scale is 10 μm for the three images). There are no portions of aluminum foil that were not covered. The coating appears more even than those on Samples 1 and 2. After three coats (c), roughness features are not as prominent as on other samples. a) 1 Coat. b) 2 Coats. c) 3 Coats. ....	35
Figure 31: 1,000X SEM Image of 1 coat of Batch # 3 of Superhydrophobic Coating on Aluminum foil. Coating and roughness features appear very similar to those on the samples obtained from the University of Illinois (Figure 22). Some portions of uncoated aluminum foil can be seen (area denoted by black arrow). Image scale is 10 μm. ....	37
Figure 32: 1,000X SEM Image of 1 coat of Batch # 3 of Superhydrophobic Coating on Smooth Glass. Sample is slightly less superhydrophobic than the other samples. Might be because some more areas of the glass surface were not coated (areas denoted by white arrows. Image scale is 10 μm.....	37
Figure 33: 1,000X SEM Image of 1 coat of Batch # 3 of Superhydrophobic Coating on Cardboard. The surface of the cardboard is not visible, indicating that either the coat was properly applied or the roughness of the cardboard surface has features similar in size to those added with the coating. This may explain why coated cardboard appears to be even more superhydrophobic than coated glass (Figure 32). Image scale is 10 μm.....	38
Figure 34: 1,000X SEM Image of 1 coat of Batch # 3 of Superhydrophobic Coating on balsa wood. This surface is also very superhydrophobic. This may be in part due to the roughness already present on the wood before coating (similar to the cardboard	

case in Figure 33). This image shows that some portions of the surface were not coated (denoted with black arrows), but it also shows how the coating has being moulded to fit the shape of the roughness features already present (white arrows). Image scale is 10  $\mu\text{m}$ . ..... 38

Figure 35: Advancing, Receding (left axis) and Hysteresis (right axis) contact angles of water for each of the coated aluminum sheet samples. Although all the surfaces are superhydrophobic, it can be seen that the samples coated with the external mixing airbrush (1 - 4) benefit from additional coats. The samples coated with the internal mixing airbrush (5 - 8) show very little change in the advancing contact angle with increased number of coats yet show and improvement in the receding contact angle. .... 39

Figure 36: Advancing, Receding (left axis) and Hysteresis (right axis) contact angles of water for each of the coated aluminum sheet samples. These samples are coated incrementally only with the internal mixing airbrush. There is a very slight increasing trend for the advancing and receding contact angles with increased number of coats. There is also a very slight decrease in hysteresis for the same incremental coating. .... 40

## List of tables

---

Table 1: List and definitions of available Roughness Parameters.....	2
Table 2: Spatial and vertical resolutions of CSM objectives used for roughness scale determination.....	29
Table 3: List of components used and their final concentration for making superhydrophobic coating .....	32
Table 4: Number and type of coating applied to aluminum sheet samples along with coat thickness, advancing, receding contact angles and contact angle hysteresis. ....	39
Table 5: Number of coats applied to aluminum sheet samples along with coat thickness, advancing, receding contact angles and contact angle hysteresis. ....	40



# 1 Introduction

---

Superhydrophobic surfaces (SHS) are naturally occurring (lotus leaves) and man-made surfaces (plasma etched PTFE) that are very hard to wet. The interaction between the water drops and these hydrophobic surfaces was first studied and documented by Thomas Young in 1805.<sup>1</sup> Generally, hydrophilic surfaces have contact angles  $\theta$  from  $0^\circ$  to  $30^\circ$ , hydrophobic surfaces have contact angles greater than  $90^\circ$  and superhydrophobic surfaces have contact angles greater than  $150^\circ$ .<sup>2</sup> These surfaces are commonly referred to as self-cleaning surfaces. The topic of superhydrophobic surfaces has gained marked interest in academic, industrial and commercial research. The focus of this research lies in fundamental research and practical manufacturing.<sup>3</sup> In particular, much of this research is geared specifically towards the development of advanced superhydrophobic surfaces, materials and coatings with practical purposes. It is fair to say that the properties of superhydrophobic surfaces and the requirements to achieve such properties are understood well and broadly thanks to the active participation of universities and corporations. However, very little knowledge has been gained on understanding the durability and robustness of these materials. It is necessary to understand how superhydrophobic surfaces change as they wear so that steps can be taken to make these surfaces a reality in production.

The goal of this research work is to study and understand how different superhydrophobic surfaces and their properties (i.e. topography, chemistry) change when they are subjected to different kinds of wear (i.e. by abrading, impacting, scratching) in order to be able to recommend on the design of such surfaces. The changes in the properties of the surfaces can be observed by studying the different surface roughness parameters and the surfaces' wetting behaviour. The surfaces' topographical and chemical properties can be altered together or independently. This can be achieved by looking at surfaces whose chemistry would not change with wear (plasma etched PTFE), surfaces whose topography would not change with wear (smooth glass coated with Teflon®) or surfaces in which both properties would be changed simultaneously (acid etched Aluminum coated with Teflon®). The information gathered from this work can be directly applied to the design of superhydrophobic surfaces and coatings so that water repellency and surface durability can be optimized (higher contact angles and longer durability).

The scope of this research work is limited to studying surfaces where topography alone as well as topography and chemistry are altered or worn. The reason for excluding surfaces in which only chemistry is changed is that it would become the study of a coating on a smooth substrate. Such smooth surfaces coated with a hydrophobic material (i.e. Teflon® on smooth glass) are not superhydrophobic since they lack the component of porosity or roughness required to achieve superhydrophobicity.<sup>4</sup>

The work has been performed in three stages and therefore the experimental details and the results gathered at each stage are presented in three separate sections:

1. Wearing Plasma Etched PTFE: focused on developing abrasive wear testing method and an initial relationship between roughness parameters and wetting behaviour.
2. Wearing Aluminum Foil coated with Superhydrophobic Coating: focused on the relationship between roughness parameters, wetting behaviour and roughness scales.

3. Developing Superhydrophobic Coating: focused on the relationship between the topographical properties, chemical properties and wetting behaviour of a superhydrophobically coated surface as well as coating techniques and their relationship to surface roughness and final superhydrophobicity.

The surface roughness data (Table 1) is collected by using a white light Confocal Scanning Microscope (CSM), high resolution surface topography images are obtained with a Scanning Electron Microscope (SEM) and wetting behaviour contact angles of water are measured with Axisymmetric Drop Shape Analysis (ADSA). Other results are qualitative in nature and based primarily on observations.

*Table 1: List and definitions of available Roughness Parameters*

<i>Linear Parameters</i>	
$R_a$	Arithmetic average roughness
$R_q$	Mean square root roughness
$R_v$	Maximum trough depth
$R_z$	Maximum height roughness
$R_c$	Average height of roughness curve element
$R_t$	Maximum section height of roughness curve element
$R_p$	Maximum crest height
$R_{sk}$	Roughness curve skewness
$R_{ku}$	Roughness curve kurtosis
$R_{sm}$	Average length of roughness
<i>Volume Parameters</i>	
$S_a$	Arithmetic mean height
$S_q$	Root mean square height of the scale limited surface
$S_z$	Maximum height of scale limited surface
$S_{sk}$	Skewness of scale limited surface
$S_{ku}$	Kurtosis of scale limited surface
$S_p$	Maximum peak height
$S_v$	Maximum trough depth
$S_k$	Difference of core level
$S_{pk}$	Reduced peak height
$S_{vk}$	Reduced valley height
$S_{mr1}$	Load area ratio separating reduced peak height and core
$S_{mr2}$	Load area ratio separating reduced valley depth and core
$V_{vc}$	Core void volume of the texture surface
$V_{vv}$	Valley void volume of the texture surface
$V_{mp}$	Material volume of the texture surface
$V_{mc}$	Core material volume of the texture surface
$S_{dq}$	Root mean square surface slope comprising the surface
$S_{dr}$	Developed interfacial area ratio

$S_{ds}$	Summit density
$S_{sc}$	Mean summit curvature
$S_t$	Maximum height of topographic surface
$S_{10z}$	Ten point height of surface

---

*Geometrical Features*

---

Volume	Volume of surface above a specified height
Surface Area	Surface area of the topography above a specified height
Maximum Peak Height	Maximum height found measured from a specified reference height
$r$	Roughness factor is the ratio of the surface roughness to the projected area of the topography
$f$	Ratio of surface area wet by liquid (above a specified height) to total surface area

---

It has been determined that under the operating conditions described in the following sections that these superhydrophobic surfaces (specifically plasma etched PTFE) can be worn sufficiently to show reduction in hydrophobicity with receding contact angles as low as 70°. It was also found that advancing and receding contact angles are not equally susceptible to wear, with receding contact angles showing higher sensibility to surface changes after wear. These changes and differences between advancing and receding contact angles (hysteresis) were compared with roughness parameters and surface topography data in order to determine the relationship between them. One parameter that stands out first is Rsk (skewness), showing significant changes in its trend that can be directly related to changes in wetting and hysteresis. Other parameters such as Ra, Rq, Rku, Sa, Sq, Ssk, Sku, r, f and Surface Area have been found to show trends or changes that can be related to wetting behaviour better than the rest. These select parameters however were shown to have different trends when looking at different roughness scales (data obtained by examining the surface roughness information at different magnifications). This information was used to determine which parameters are and which are not affected when processing different roughness scales. This provides a more comprehensive understanding of how to interpret the different roughness parameters between different superhydrophobic surfaces since these surfaces will most likely have different substrates, coatings or roughness scales (i.e. Teflon® coated aluminum roughened through acid etching versus smooth glass coated with superhydrophobic coating made with nano-particles).

In the following sections, additional details are provided about the different parts, experimental methods, results obtained and conclusions the conclusions drawn from such results.

## **2 Wearing Plasma Etched PTFE**

---

### **2.1 PHASE I**

#### **2.1.1 Experimental Details**

The first phase of the experimental work conducted on wearing Superhydrophobic Surfaces (SHS) was divided in three main parts: 1) Experimental set-up and feasibility investigation, 2) Preliminary experiments, observations and qualitative analysis and 3) Experimental work with complete quantitative data collection and analysis. The goals for the different parts are to:

- Successfully set-up and abrading experiment.
- Determine optimum running experimental conditions for Plasma Etched PTFE.
- Gather data and establish relationships between surface properties and wetting behaviour.

##### **2.1.1.1 First Part: Experimental Set-up and Feasibility Investigation**

The First Part centered on the investigation of practical abrading materials, abrading conditions and experimental feasibility analysis for plasma etched PTFE and acid etched (coated and uncoated) Aluminum. Other wear tests have also been considered and are still under investigation. Examples of other tests are impact and scratching tests and are discussed later in this report. The initial goal was to be able to successfully set up an abrading experiment that would allow the following:

- Control over how much wear a surface was subject to.
- Random wear pattern (non-directional).
- Consistent results (repeatability).
- Little to no contamination of samples tested.
- Ability to choose abrading material (i.e. sand particles, glass beads, etc.)

Based on these initial requirements, the experiment was designed around standard test specification ASTM F735-06 (Standard Test Method for Abrasion Resistance of Transparent Plastics and Coatings using the Oscillating Sand Method). It was decided that this standard was appropriate for superhydrophobic surfaces since some of them are indeed coated (i.e. Teflon® coated acid etched Aluminum or superhydrophobic coating coated samples) or posses qualities similar to coated samples (i.e. Plasma Etched PTFE). Based on the details given in the ASTM standard, it was decided that these superhydrophobic surfaces would be placed flat at the bottom of a recipient with abrading material covering the surface. Whichever abrading material is used should move in a random motion parallel to the surface. The motion of the material should be easily controlled (i.e. cycles per minute or revolutions per minute) and the material and its amount should be easily changed (i.e. material volume or material height).

To perform this experiment, and for close resemblance to the ASTM standard, a Gyrotory Shaker made by New Brunswick Scientific Co. (model G2) was selected. The shaker moves in circular

motion, has a dial that controls rpm from 0 to 500 and is originally designed with a flat top where usually glassware containing a particular substance is placed. Shakers like these have been used to stir substances but are currently being replaced by magnetic stirrers. Having obtained this particular gyratory shaker, it was modified to fit our experimental plan and the standard. A tray with a capacity to hold up to 3200 mL (10" L x 10" W x 2" H) of abrading material was made and attached to the shaker. This tray is slotted at the bottom to fit samples (1 3/4" x 1 3/4") flush with the tray so that the sample's edges do not interfere with the abrading material.

The abrading materials considered were sand particles and glass beads. These abrading materials conform to the initial specification of the standard and are materials commonly used for eroding manufacturing processes as well as for sandblasting. Both of these materials are obtained easily and inexpensively. Initial testing of these materials rendered them adequate for testing purposes, therefore no other abrading materials have been considered since. Each of these materials was tested and yielded different results:

a. Sand Particles

- ◆ Particles are very irregular in shape and size.
- ◆ Generally brown in color.
- ◆ Very abrasive, making it more difficult to control proper amount of wear desired.
- ◆ Surfaces contained dirt/impurities after being worn and even after being cleaned making the white Plasma Etched PTFE samples were light yellow to light brown in color.

The following figures show the topography of Plasma Etched PTFE unworn (Figure 1), worn for 5 minutes at 300 rpm and uncleaned (Figure 2) and worn for 5 minutes at 300 rpm and cleaned (Figure 3).

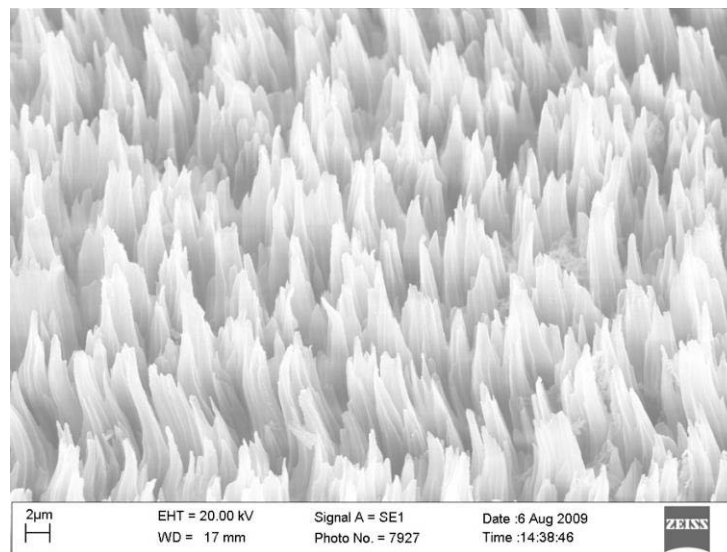


*Figure 1: SEM Image of unworn Plasma Etched PTFE. The roughness and pillars can be clearly observed. Image scale is 2 µm.*

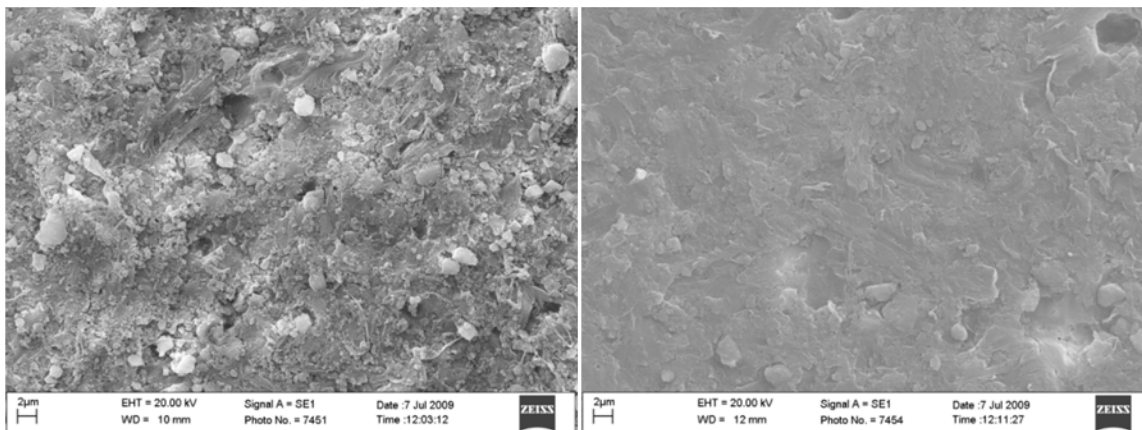


*Figure 2: SEM Image of Plasma Etched PTFE sample after being worn with sand. The sample has not been cleaned after wearing and shows the presence of small sand particles roughly 2 µm in size. Image scale is 2 µm.*

*Figure 3: SEM Image of Plasma Etched PTFE sample after being worn with sand. The sample has been cleaned in an ultrasonic bath after wearing and still shows the presence of small sand particles roughly 2 µm in size. Image scale is 2 µm.*

The irregular shape of the sand particles can be observed on Figure 2 and Figure 3 their presence even after ultrasonically cleaning the samples in ethanol following the procedure described in Annex A. It can also be observed that the abrading conditions used (5 minutes at 300 rpm in ½ inch of glass bead height) change the topography of the surface dramatically. This leads to the investigation of the second abrading material: glass beads.

b. Glass Beads

- ◆ Particles are more uniform in shape and size (roughly spherical).
- ◆ Colorless/Transparent.
- ◆ Not as abrasive as sand, therefore allowing more control over amount of wear desired.

Samples show little to no contamination after being ultrasonically cleaned in ethanol.

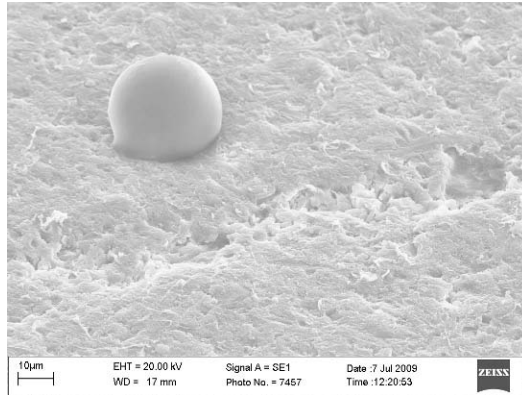


*Figure 4: SEM Image of Plasma Etched PTFE sample after being worn with glass beads. The sample has not been cleaned after wearing and shows the presence of one glass bead roughly 25  $\mu\text{m}$  in diameter. Notice there is no contamination visible on the rest of the image. Image scale is 10  $\mu\text{m}$ .*

It can also be seen from Figure 4 that glass beads can induce an amount of wear that goes beyond the requirements of the experiment since the sample shown is no longer superhydrophobic based on wetting observations.

Although it was seen that sand particles proved to be sufficiently abrasive for the experiment (they can wear the surface beyond our requirements), it was determined that they were too aggressive, limiting the amount of control over how much surface can be worn. Figures 2 and 3 show that the surface is not only worn but also torn, generating a new roughness on the sample that would alter any data collected through characterization (i.e. roughness parameters and wetting behaviour). The sample worn with glass beads in Figure 4 shows a less violent form of abrasion (no significant amount of tearing, mostly just leveling of the roughness features). The sand particles used also left traces on the sample (therefore becoming part of the roughness) changing the wetting behaviour. It was mainly for these reasons that glass beads were chosen as the appropriate medium to wear the PTFE samples allowing the experiment to better reach the initial goal and requirements.

#### **2.1.1.2 Second Part: Preliminary Experiments, Observations and Quantitative Analysis**

The Second Part focused on test runs of the experiment in order to determine the adequate wearing conditions for PTFE. The factors that would influence the wearing conditions, as established in the ASTM standard and as mentioned in the First Part, are shaker rpm (velocity/energy of particles abrading the surface), amount of abrading material (height/volume of material) and wearing interval (length of time a sample is subject to wear).

It was determined that the experimental set-up allows for sufficient wear of both Plasma Etched PTFE as well as Acid Etched Aluminum. The goal is to be able to fine tune the operating conditions such that changes in the wetting behaviour of the surface can be observed and captured with the different characterization techniques used (CSM, SEM, ADSA). Figure 5 and Figure 6 show the unworn and worn acid etched Aluminum samples respectively.

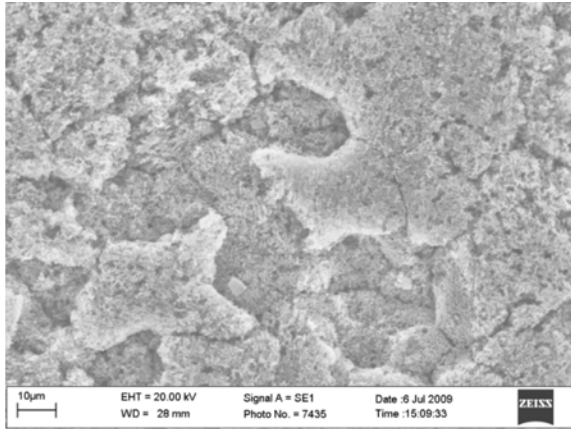


*Figure 5: SEM Image of unworn Acid Etched superhydrophobic Aluminum shows various levels of roughness. Image scale is 10 μm.*

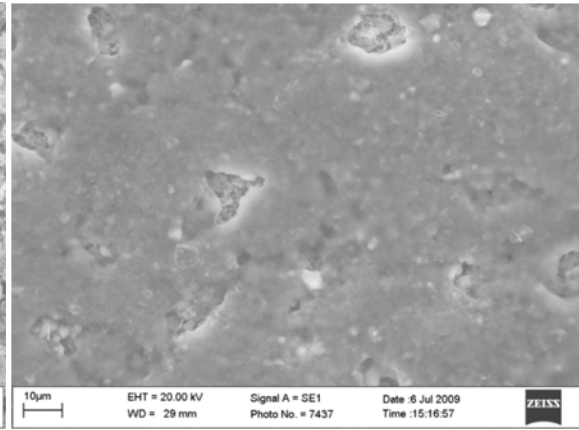


*Figure 6: SEM Image of an Acid Etched superhydrophobic Aluminum sample worn with glass beads for 5 minutes at 300 rpm. Sample has lost most of its roughness and is no longer hydrophobic. Image scale is 10 μm.*

It was determined that ½ inch of glass bead height running at 300 rpm for 30 second intervals was excessively abrasive for Plasma Etched PTFE. It was also found that less than 200 rpm was not sufficient to generate a significant amount of wear due to very limited relative motion between the glass beads and the shaker tray (<0.5 cm). Such small relative motion would not change the topography and the wetting behaviour of the surfaces. To start, 200 rpm were chosen as the bare minimum for wearing the plasma etched PTFE. This setting maximized the amount of time a sample would transition from one wetting result to another, allowing us to properly capture the transition points between superhydrophobic ( $\theta > 150^\circ$ ), hydrophobic ( $\theta > 90^\circ$ ) and no longer hydrophobic ( $\theta < 90^\circ$ ) behaviour.

From this experimental work, a standard operating and wearing procedure was developed for appropriately wearing (allowing for observation of changes in wetting behaviour) and characterizing plasma etched PTFE samples and is included in Annex B. The procedure is generic and can be applied for different superhydrophobic materials. Changes and adjustments to rpm, abrading material height/volume and wearing time interval are required for every different superhydrophobic material.

### **2.1.1.3 Third Part: Experimental Work with Complete Quantitative Data Collection and Analysis**

The Third Part was the complete experimental work with quantitative data collection based on the final conditions established from the Second Part. The goal of this experimental work was to better understand the relationship between the roughness parameters and the wetting behaviour of the samples. Each of the samples studied underwent characterization with different methods. Roughness parameters were obtained by using white light Confocal Scanning Microscopy (CSM), surface topography was obtained by using Scanning Electron Microscopy (SEM) and wetting behaviour was obtained by using Axisymmetric Drop Shape Analysis (ADSA).



The relationships between the surface properties and the wetting behaviour were made primarily by examining the trends in the various roughness parameters mentioned in Table 1 and relating them to the trends seen in the wetting data gathered. Both results (roughness parameters and wetting data) were then compared to the topography of the surface (qualitative SEM Images) in order to better understand how the physical changes on the surface dictate the quantitative data gathered with CSM and ADSA.

The first experimental results were collected after wearing a Plasma Etched PTFE sample at 200 rpm for a glass bead depth of 1/2 inch at 30 second wearing intervals. These conditions allowed for the observation of a transition in wetting. As shown in Figure 2.7, there is an increasing change of hysteresis with increased wear time can be clearly observed (starting between 3 and 3.5 minutes of wear). It is worth noting that the advancing contact angle remains roughly superhydrophobic (lowest at 7.5 minutes for 146°) while the receding contact angle continues to decrease to 68°, well below the hydrophobic regime. This behaviour is observed with ADSA as pinning of the drop as it recedes. The term ‘pinning’ is used to describe the scenario when a water drop is receding on a surface, but the contact radius of the drop remains the same while the contact angle is decreasing.<sup>5</sup>

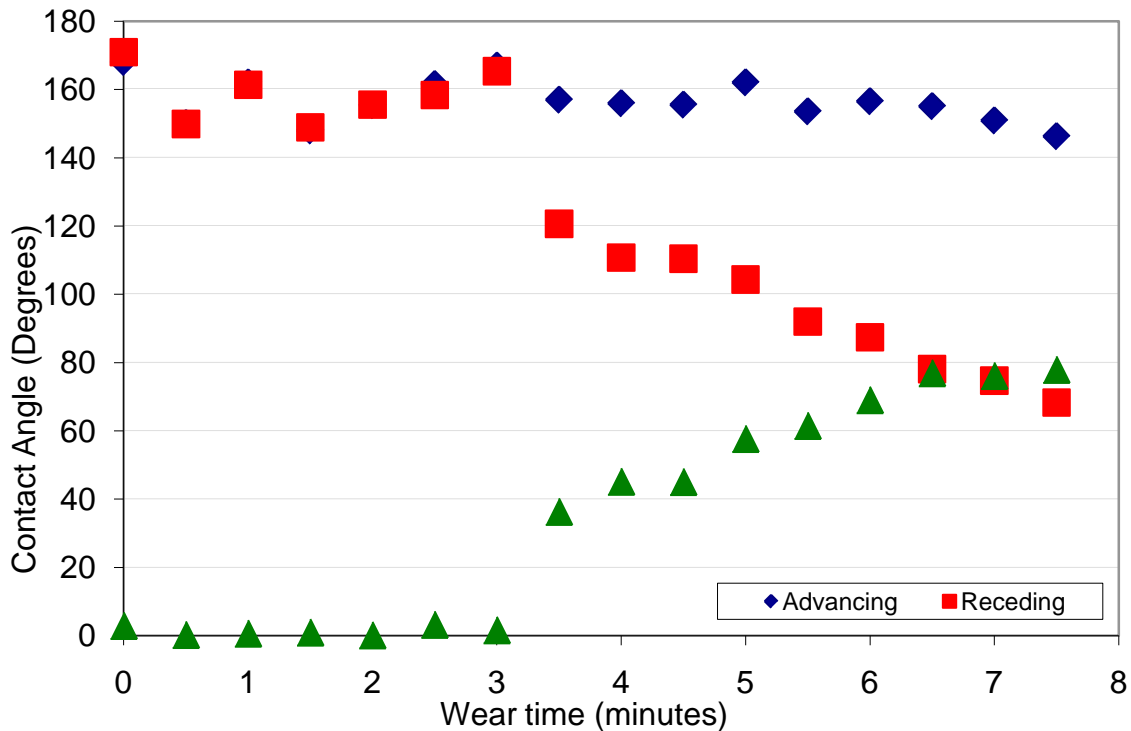


Figure 7: Advancing, Receding and Hysteresis contact angles of water vs. wear time for Plasma Etched PTFE. A decreasing Receding contact angle can be seen as wear time increases. The difference between the Advancing and the Receding contact angles is plotted as the Hysteresis. This difference is observed as pinning of the drop when it is receding. Sample was worn at 200 rpm with 1/2 inch glass bead depth in 30 seconds wear intervals.

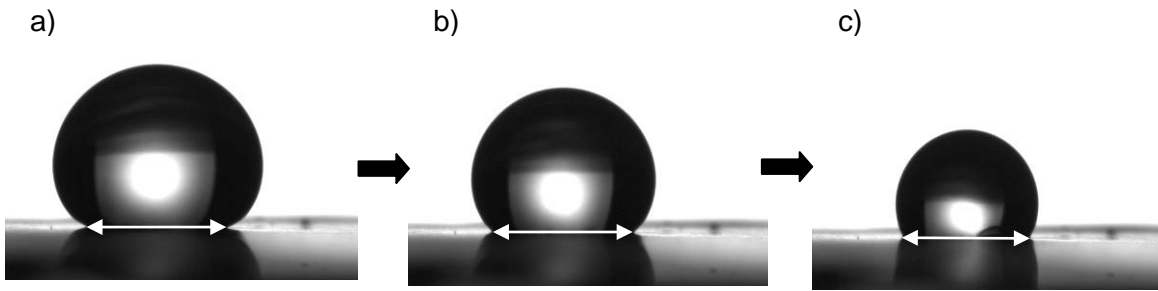


Figure 8: A water drop receding across a worn Plasma Etched PTFE sample. The water drop is receding from a) to c). This transition is defined as “pinning” as the points where the drop contacts the surface remain at the same place (constant contact radius) with a decreasing receding contact angle. The white line in the images is a constant length throughout and is just a reference line to show a constant contact radius.<sup>5</sup>

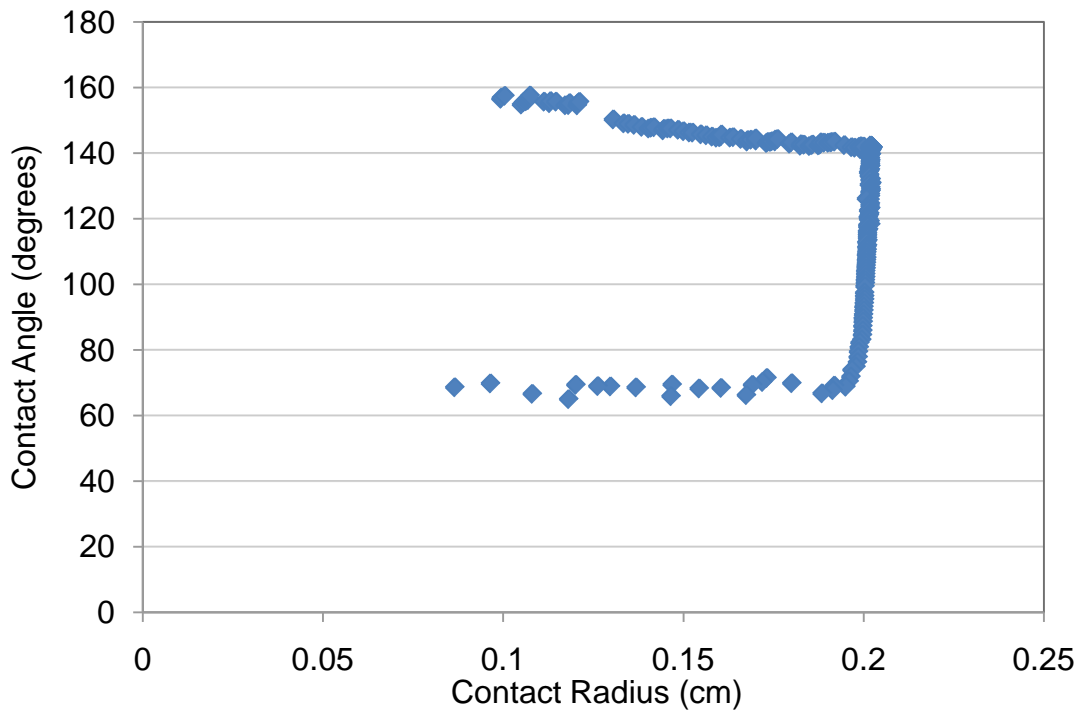


Figure 9: A plot of contact radius against the contact angle as a water drop is first advancing, then pinning, and then receding across a worn plasma etched PTFE sample. During the pinning transition, the contact radius remains fairly constant while the contact decreases until the water droplet starts receding at a lower contact angle.<sup>5</sup> Sample worn at 200 rpm with 1/2 inch glass bead height at 30 seconds wear intervals.

Although the increase in hysteresis has been captured through wetting analysis, it is not clear where the onset of this pinning starts. This means that the experimental operating conditions have to be tuned further to better capture the transition point (pinning behaviour) from low to increasing hysteresis. Nonetheless, these initial results were sufficient to start developing the fundamental basis of the relationship between changes in roughness and wetting. Out of the 37 relevant roughness parameters defined in Table 1, 13 of these parameters were selected as the ones that show a closer relationship between the changes in roughness properties and wetting behaviour based on observations of their trends. Four parameters relate to linear data: Ra, Rq, Rsk and Rku. Six parameters relate to volumetric data: Sa, Sq, Ssk, Sku, Sdr and Sds. Three parameters relate to geometrical features: Surface Area, r and f. The parameters Sa, Sq, Ssk and Sku are the volumetric counterparts of Ra, Rq, Rsk and Rku. The parameters Sdr, Surface Area, r and f are all based on a relationship between the developed (rough) surface area and the projected (planar) surface area. Of particular interest for the first experiments are the parameters Rsk and Ssk (linear and volumetric parameter related to skewness) shown in Figure 10.

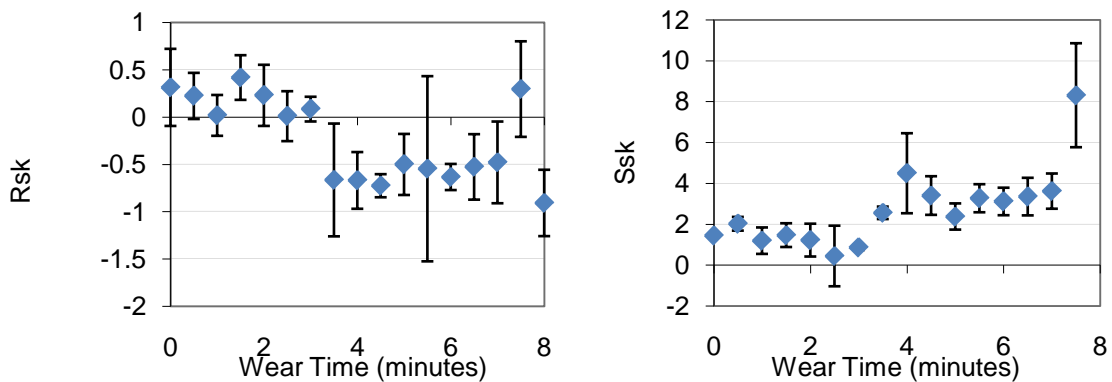


Figure 10: Plot of skewness parameters (Rsk left and Ssk right) for Plasma Etched PTFE sample worn at 200 rpm 1/2 inch of glass beads at 30 second intervals. This parameter shows a jump between 3 and 3.5 minutes (with relatively constant values before and after). This is the same sudden change seen for the wetting data in Figure 7.

The skewness parameters are defined as the measure of the 2-D and 3-D skewness of a surface and are used to quantify the symmetry of a surface along a line of cross section. When skewness is negative, it means that the surface consists of deep valleys instead of tall peaks, while positive skewness is the opposite.<sup>5</sup> The jump seen with Rsk and Ssk shows the clearest relationship to the wetting data in the sense that these parameters show similar values before water drop pinning and different magnitude yet similar values after drop pinning. In the case of Rsk, positive parameters are seen before the pinning behaviour and negative values after the pinning behaviour starts. The fact that these parameters show a good relationship to the wetting results does not mean that the other parameters are ineffective. For example, the surface parameters also show a trend that can be closely related to the wetting behaviour. Figure 11 and Figure 12 show the trends of the non-dimensional r parameter (roughness area to projected area ratio<sup>6</sup>) and the non-dimensional Sds parameter (summit density) with increased wear time.

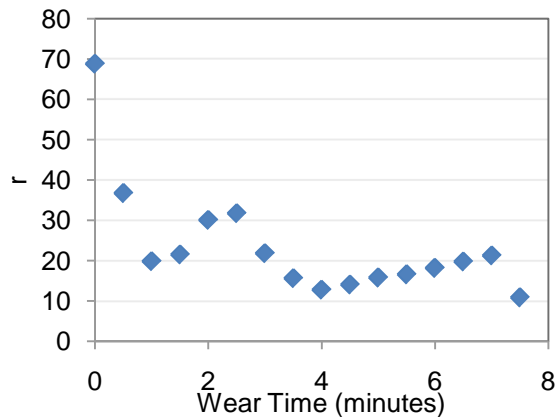


Figure 11: Plot of the  $r$  parameter for worn Plasma Etched PTFE sample shows a sharp decrease in rough surface area with increased wear time.

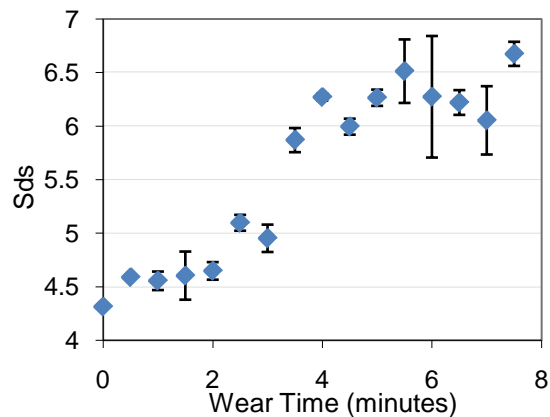


Figure 12: Plot of the  $S_{ds}$  parameter for worn Plasma Etched PTFE sample shows an increasing trend with wear time and also captures the sudden change in wetting at 3-3.5 minutes.

It can be said that not a single parameter would accurately and singularly replicate the trend observed for the wetting behaviour, instead, a combination of relevant parameters would be most appropriate. To be able to interconnect the different parameters, more data needs to be collected from different surfaces to be able to adequately understand the physical implications of each of the roughness parameters as they change with wear. This requires more time to test more samples and is currently part of an ongoing investigation.

The experiment was carried out three more times under different conditions in order to better understand the mechanics of the surface wear and to better capture the transitions in wetting behaviour. The results and discussion are reported separately in “Summary of Wear Test on Superhydrophobic Surfaces”.<sup>5</sup> The experimental conditions used are summarized below:

1. 260 rpm, ½ inch glass bead depth at 5 seconds, 10 seconds and 20 seconds wear intervals: Focused on speeding up the experiment and studying the effect of increased speed.
  - Surfaces exhibited pinning after the first wear interval.
  - 260 rpm is more aggressive than what is required to meet the experimental goals.
  - Three different iterations showed good consistency in wetting behaviour.
2. 200 rpm, ½ inch glass bead depth at 30 seconds wear intervals: Focused on replicating the initial experimental data described in the Third Part of Phase I.
  - Adjustments made to the shaker (changed belt) made test more aggressive than before due to increased energy transfer efficiency.

3. 175 rpm with ½ inch glass bead depth and 187.5 rpm with 1 inch glass bead depth at 30 seconds wear intervals: Focused on reducing the amount of wear in order to be able to capture the onset of the transition point in wetting behaviour as well as investigating the energy threshold for causing sufficient wear on the surface.

- Speeds were chosen as they exhibited very slight relative motion of glass beads to shaker tray.
- Surfaces were worn although not enough to show changes in wetting.

## 2.2 PHASE II

The second phase of the experimental work focused on replicating the results obtained in Phase I with more precision in the measurements taken and the procedures followed. The goal of this experimental plan centers on the continuation of Phase I with specific focus on the following topics:

- ♦ Capturing drop pinning behaviour (change in contact angle hysteresis)
- ♦ Further studying the relationship between roughness parameters and wetting behaviour.
- ♦ Exploring the possibility of a combination of different roughness parameters to explain changes in surface wetting.
- ♦ Exploring energy thresholds (how much energy is required to wear the surface a particular amount)

The experimental work was conducted by performing incremental wear on an unworn Plasma Etched PTFE sample at 195 rpm in 1 inch of glass bead depth and at 30 seconds wear. In between the wear intervals, the sample was characterized with the CSM for roughness parameters, SEM for surface topography and ADSA for wetting behaviour. The higher speed of 195 rpm was chosen over the 187.5 rpm used last in Phase I because 187.5 rpm proved to be inadequate for wearing the PTFE sample adequately.<sup>5</sup> 195 rpm might break the energy threshold found at 187.5 rpm and still capable of yielding less aggressive results than those obtained at 200 rpm after changing the shaker's belt.

The surface of the PTFE sample was worn at the 195 rpm indicated with little to no change in hysteresis for up to 120 (2 minutes) seconds as seen in Figure 13. From 150 seconds to 180 seconds (2.5 - 3 minutes), some slight pinning was observed in the receding phase with ADSA at high water recharge volume rates (2 µL/s default rate compared to 0.5 µL/s experimental rate). This higher volume rate of 2 µL/s is used when manually adjusting drop volume when setting up the software before capturing data; however, when conducting the wetting test and gathering data at 0.5 µL/s, little change in hysteresis was noticed. It has been determined that around 120 - 150 seconds of wear (2 - 2.5 minutes), is the point that marks the onset of the pinning behaviour in receding most clearly described with Figure 7 in Phase I. The drop continued to pin very slightly at the higher default water volume rate of 2 µL/s (used when adjusting the software for data capturing) up to 300 seconds of wear (5 minutes). At this point, a significant change in hysteresis (10.07°) was observed and captured as can be seen in Figure 13 and Figure 14.

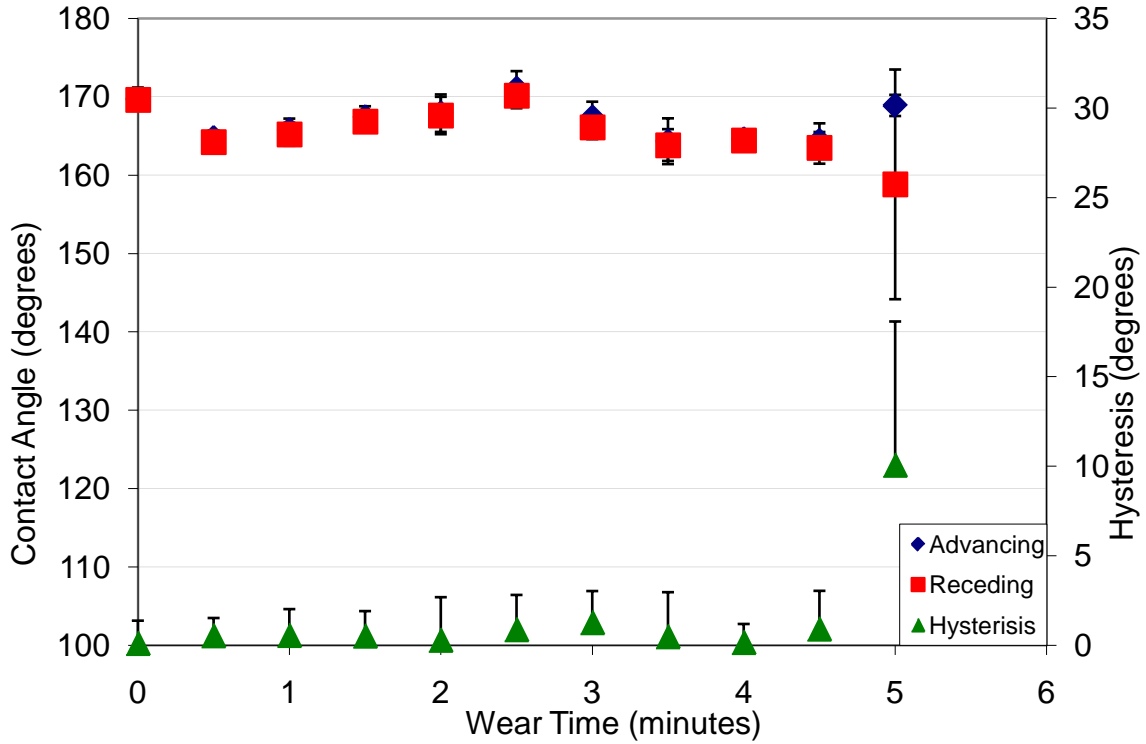


Figure 13: Contact Angles of water with Wear Time (in minutes). Contact angle on the left axis and hysteresis on the right axis. This figure clearly shows little to no change in hysteresis for a total of 270 seconds (4.5 minutes) of wear time. At 300 seconds (5 minutes), a clear jump in hysteresis is observed marking the beginning of the pinning behaviour shown in Figure 14. Sample was worn at 195 rpm in 1 inch of glass bead depth at 30 seconds intervals.

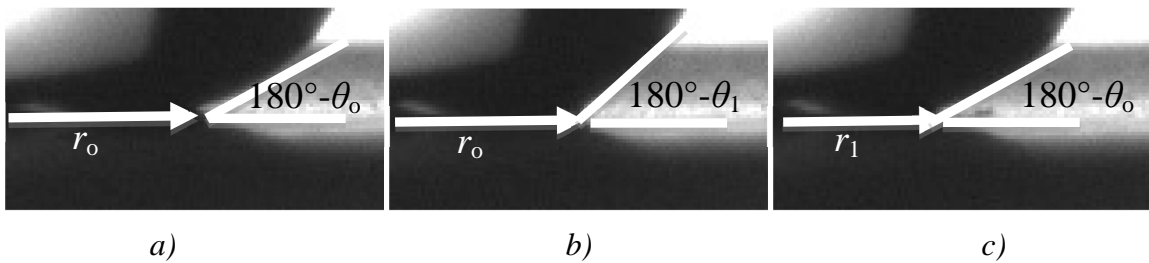


Figure 14: Pinning behaviour of water drop in the receding phase of the wetting test. This behaviour is indicative of the surface starting to lose its superhydrophobicity. a) Before pinning with contact radius  $r_0$  and receding at a contact angle  $\theta_0$ . b) Last frame of pinning behaviour with the same contact radius  $r_0$  from 'a' but a lower contact angle  $\theta_1$ . c) Right after releasing from pinning with drop receding at a lower contact radius  $r_1$  than 'a' and 'b' but at the same contact angle  $\theta_0$  as from 'a'.

Although the pinning is very slight and sporadic in this surface after 300 seconds of wear, it establishes the beginning of the pinning behaviour even though the surfaces remain superhydrophobic with both advancing and receding contact angles greater than 150°.

The surfaces were fully characterized with CSM by collecting data for all the available parameters. Special focus was given to the 14 parameters described in Phase I. For this wear scenario, the two parameters that show the most interesting trends in relationship to wetting behaviour are Ssk (volumetric counterpart of Rsk described in Phase I) and r (roughness area to projected area ratio) as shown in Figure 15 and Figure 16, respectively.

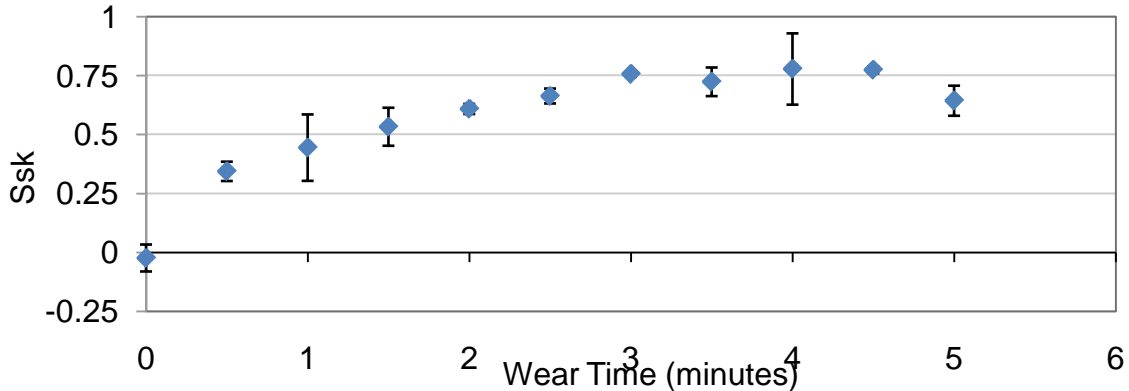


Figure 15: Plot of the non-dimensional Ssk parameter (volumetric skewness) vs. Wear Time shows an increasing trend with observed pinning for a Plasma Etched PTFE sample worn at 195 rpm in 1 inch of glass bead depth at 30 seconds wear intervals.

The Ssk parameter (volumetric skewness) turns out to be of particular interest again this time, showing an increasing trend from a value of -0.02 for the unworn sample to a value of 0.77 for the sample worn for 270 seconds (4.5 minutes). At 300 seconds (5 minutes), a slight drop in Ssk to a value of 0.64 can be seen. This change in volumetric skewness reflects the change in wetting behaviour where at 300 seconds a sudden increase in hysteresis is observed.

Another parameter that reflects the changes made to the surface by subjecting it to wear it is the r parameter shown in Figure 16. The total developed surface area due to the roughness and structure of the pillars is seen decreasing with increasing wear time, meaning that there is not so much material/surface available as a first point of contact for the water drops. Wenzel<sup>7</sup> described the relationship between the roughness of a surface through parameter r and the surfaces wetting behaviour through Equation (1):

$$\cos \theta_{app} = r \cos \theta_Y \quad (1)$$

where  $\theta_{app}$  is the apparent contact angle (experimentally accessible angle) and  $\theta_Y$  is the Young's contact angle (the angle related to the solid surface energy observed on a smooth surface).<sup>1,6</sup>

Out of the various parameters obtained from CSM, the f parameter (ratio of surface area wet by liquid to total surface area) should also be a good indicator of the changes in behaviour. This parameter is better described by the Cassie-Baxter model as shown with Equation (2):

$$\cos \theta_{app} = r \cdot f \cos \theta_Y + f - 1 \quad (2)$$

where if  $f = 1$ , the Cassie-Baxter equation becomes the Wenzel equation.

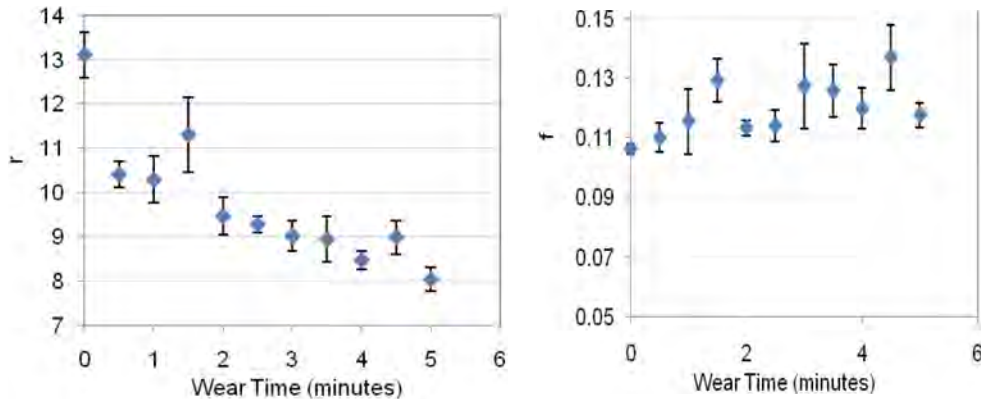


Figure 16: Plots of the surface area ratio ( $r$  parameter) and the ratio of solid surface area wet ( $f$  parameter) vs. wear time. The plot for  $r$  shows a decreasing trend with increasing wear time reaching its lowest point at 300 seconds (5 minutes) of wear, also the same point at which hysteresis is highest. The plot for  $f$  however, shows a very slight increase in surface area wet by the liquid, yet not a strong enough trend to directly connect to wetting. Plasma Etched PTFE sample worn at 195 rpm in 1 inch of glass bead depth at 30 seconds wear intervals.

For this particular experiment, the  $f$  parameter has been calculated for the peaks above the 90<sup>th</sup> percentile of the distribution of heights for all the available surface peaks. The  $f$  parameter should show an increasing trend with wear. The reason being that as wear increases and the tallest peaks are worn down, more peaks become available to make contact with the liquid, therefore increasing the adhesion of a drop of liquid to the surface (decreasing contact angle).

Although the changes in contact angles (advancing and receding) are not very significant for the first 270 seconds of wear (4.5 minutes) as seen in Figure 13, it does not mean that nothing is changing in the surface's topography. This particular experiment has been able to show that, even though the wetting data for the Plasma Etched PTFE sample does not show large variations or discrepancies (contact angles vary by  $\sim 2^\circ$  on average), the roughness parameters clearly show quantifiable changes that are reflected in the trends of parameters such as  $S_{sk}$  and  $r$  as described with Figure 15 and Figure 16.

Even though there might exist a combination of parameters that may properly describe the wearing process of a given surface as described in Phase I, it is necessary to gather more data on the different roughness parameters and how each parameter relates to changes in surface topography as well as wetting behaviour. Out of the 14 relevant roughness parameters initially selected,  $R_a$ ,  $R_q$ ,  $S_a$  and  $S_q$  still show very slight variations in their trends, making it hard to determine if they might be able to properly describe the effects of wear on a surface. Being able to select parameters such as  $S_{sk}$  and  $r$ , allow for a better understanding on how the other relevant



parameters are affected by or related to wear, enabling the development of a much tighter simultaneous relationship (or linear combination) with the remaining roughness parameters.

This experimental work has also established the conditions by which the onset of the pinning behaviour is captured (195 rpm in 1 inch of glass bead depth at 30 second wear intervals), providing us with the data required to estimate the amount of mechanical energy necessary to reach the transition point in wetting for this particular surface.

The details of the experimental work and the results obtained are included in the report “Studying the Wear of Superhydrophobic Surfaces: Superhydrophobic Plasma Etched Teflon”.<sup>8</sup>

## **2.3 PHASE III**

The third phase of the experiment is designed to subject the samples to different types of wear:

- Impact by dropping weight (see Annex C: Drop Weight Wear Testing Procedure)
- Scratching of the surface

The procedure and its conditions have been preliminarily determined and are yet to be implemented. The focus is to understand how a different method of wearing these surfaces might affect the wetting behaviour. It may also expose some roughness parameters that are more sensitive to impact or scratching of the surface than abrasive wear. If that is the case, the results from this phase may be connected to the results from Phase I and Phase II, allowing for a deeper understanding of the relationships between surface properties and wetting.

### **3 Wearing Aluminum Foil Coated with Superhydrophobic Coating.**

---

Two Aluminum samples were obtained from the University of Illinois in December 2009. Both of these samples were coated with their own developed wear resistant superhydrophobic coating.<sup>9</sup> The difference between the two samples was that one sample was unworn while the other sample had already been worn by the action of stomping on it. The letter describing the superhydrophobic coating shows in Figure 5b a sequence of images and a link to the video describing the action and effect of stomping on a surface coated with this coating,<sup>9</sup> it however does not match the information that accompanied the samples. In the information that came with the samples, it was described that the worn sample had been used as a mat in the department where their research is conducted. There was no specific information on the actual conditions that the second sample (worn) was subject to (i.e. weight/load, direction of wear, covered or uncovered, etc) and it cannot be assumed that it was subject to the same wear shown and described in their published letter. Both samples however, show remarkable superhydrophobicity through observation of the behaviour of water on their surface.

The goal of this experimental work is to test the toughness of the superhydrophobic coating in the context of the methods used in Section 1. More specifically:

- To analyze roughness data of the coating for the two samples before further wear.
- To subject the already worn sample to abrasive wear as described in Section 1 for comparison with the results obtained by conducting wear on Plasma Etched PTFE.
- To compare the differences in topography before and after wear between the two samples and also with the PTFE samples from Section 1.
- To identify changes in the wetting behaviour and their relationship to the topography and roughness parameters.

#### **3.1 PROCEDURE**

The procedure followed for wearing and characterizing these samples is very similar to the procedure used in Section 1 and is detailed as follows:

- A) Characterize with CSM and SEM before wearing the samples further.
- B) Wear the already worn sample (sample 2) in three different ways:
  1. By rubbing the sample by hand against a relatively smooth painted metallic surface until a change in wetting was observed: preliminary evaluation of how tough the coating was.
    - a. 80 unidirectional strokes against the surface.
    - b. Low to medium force applied by hand.

2. By rubbing the sample by hand against itself until a change in wetting was observed: preliminary evaluation of how tough the coating was.
    - a. 40 unidirectional strokes against itself.
    - b. Low to medium force applied by hand.
  3. Methodically by using the abrasive wear tester described in Section 2, Phase 1 until a change in wetting was observed.
- C) On the already worn sample (part B.1.) complete CSM and SEM data was obtained.
4. Collected data on all the roughness parameters and focused on those relevant to wear and wetting as established while wearing Plasma Etched PTFE in Section 2.
  5. Used different magnifications with the CSM to expose and identify different roughness scales and their change from one sample to the next (i.e. effective increase in wear).

## **3.2 EXPERIMENTAL DETAILS**

### **3.2.1 First Sample - Unworn:**

Although there were no wetting tests conducted with ADSA on the sample, on an initial wetting observation (informal inspection), it behaves in the same manner as superhydrophobic surfaces. Water drops of virtually all sizes are easily shed from the surface due to gravity, inertia and airflow. It is not clear from initial testing whether water drops can bounce off the surface since the aluminum foil can deflect and absorb some of the kinetic energy of the falling water drops.

Figure 17 shows how water sits on the first sample. The pictures were taken for the sample laying flat since very slight inclinations would cause the drop to roll off the surface. It was clearly noticed from wetting observations that the surface was as hydrophobic as unworn Plasma Etched PTFE and Teflon® coated Acid Etched Aluminum.

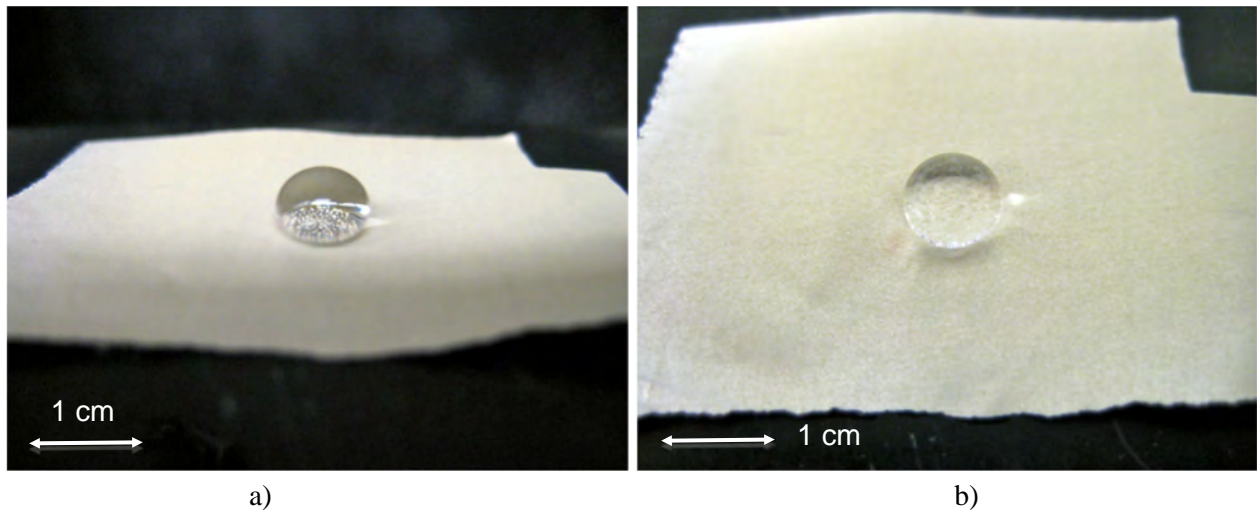


*Figure 17: Water drop laying on a flat sample of unworn aluminum foil coated with superhydrophobic coating. a) Side view. b) Angled view. It can be clearly observed that the drop is somewhat spherical in shape (despite its volume) with a circular contact area and high contact angle. Once this surface became slightly tilted, any water drops would immediately roll off.*

The SEM and CSM data containing surface topography and surface roughness information will be presented later in the report.

### **3.2.2 Second Sample - Worn by stomping from using as mat:**

According to the information that came with the samples when received, this sample was worn by stomping while being used as a mat in an area with some traffic in the department where the coating's research took place. Although there is some description as well as a video of similar action performed on aluminum foil coated with superhydrophobic coating,<sup>9</sup> there is no other information on how this was accomplished (i.e. load, frequency, length of time, etc.).

Although there were no wetting tests conducted on the sample with ADSA, on various wetting observations, it still seems to behave in the same manner as the first sample (unworn). As well as with the first sample, water drops of virtually all sizes are easily shed from the surface due to gravity, inertia and airflow. Some smaller drops do seem to get caught briefly in the various creases present on the surface (see Figure 18c) yet not enough to have a significant impact on overall wetting behaviour. It is also not clear from initial testing whether water drops can bounce off the surface since the aluminum foil can deflect and absorb some of the kinetic energy of the falling water drops.

Figure 18 shows how a water drop behaves on the second sample. The pictures were taken for the sample lying flat since very slight inclinations would cause the drop to roll off the surface. It can also be seen on these pictures the wrinkles on the surface as well as yellow specks (circled) that are not as visible on the first sample.

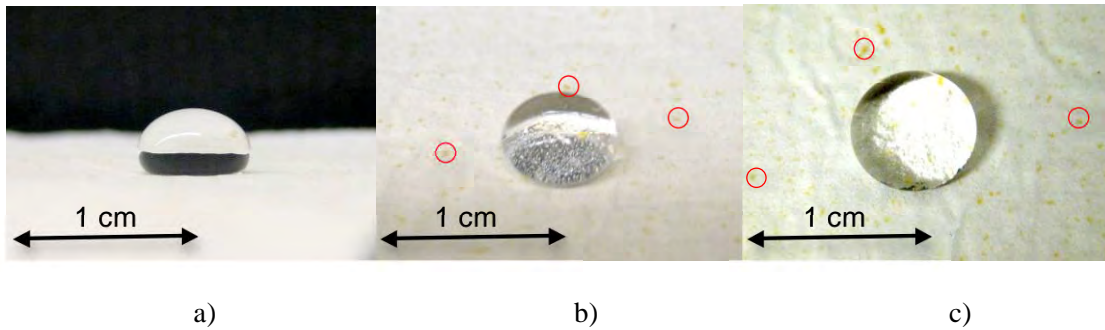


Figure 18: Water drop laying on a flat sample of stomped aluminum foil coated with superhydrophobic coating. Sample appears to be as superhydrophobic as the first. Some yellow specks not visible in the first (unworn) sample are circled. a) Side view. b) Angled view c) Top view.

The SEM and CSM data containing surface topography and surface roughness information will be presented later in the report.

### 3.2.3 Third Sample - Worn by stomping from using as mat + 8 minutes on shaker:

This sample was worn by wearing it for a total of 8 minutes in the shaker used in Section 2 at 250 rpm in 1 inch glass bead depth following the procedure in Annex B. The sample was worn 1 minute at a time until a change in behaviour and/or contact angle was observed.

Although no wetting tests were conducted with ADSA, the water drops on the third surface have a lower receding contact angle as shown in Figure 19. The first indication of such observation was that when the surface was tilted slightly ( $\sim 10^\circ - 15^\circ$ ), the drop would not immediately roll off. Instead it would hang (pin) briefly by its trailing edge before rolling off in what could be called a superhydrophobic manner (without leaving a trail of water behind). This is initially noticed by seeing that the drop does not roll off the surface while maintaining its circular contact area. Instead, the contact area is more elliptical while moving and in the shape of a teardrop while pinning. This can be observed in Figure 19 by the drop having a higher advancing contact angle and a lower receding contact angle (contact angle hysteresis) matching the results and wetting data obtained for worn Plasma Etched PTFE as described with Figures 7, 9 and 13.

Figure 19 also shows the presence of small drops that did not roll off the surface when tilting it as easily as they did with the first and second samples. This means that the force on the smaller drops from pinning is at least sufficient to keep them from effectively rolling off. Also interesting to note from the behaviour of water drops on the third sample shown in Figure 19, is that the air pockets present between the surface roughness and the water drop can be seen. This is the wetting model described by Cassie-Baxter<sup>4</sup> in which a liquid sits on top of the peaks of the surface roughness with air trapped between the valleys of the roughness and the bottom side of the liquid described with Figure 20.

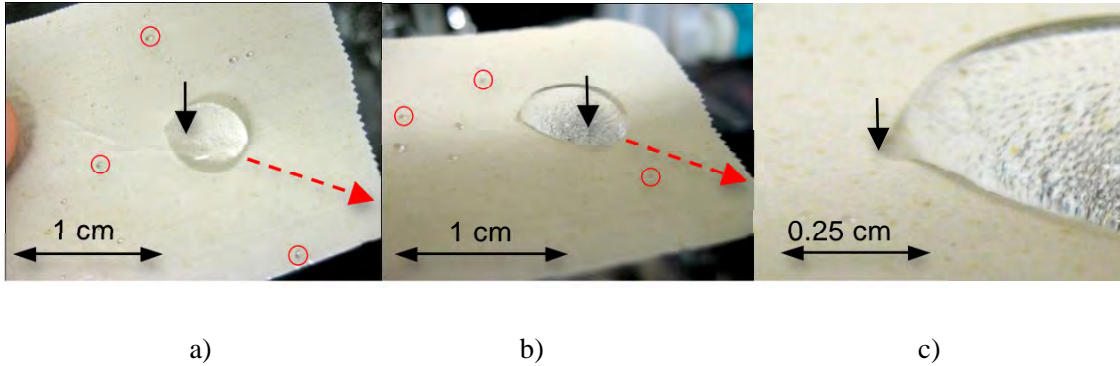


Figure 19: Water drop on third sample when tilted at a slight angle ( $\sim 10^\circ - 15^\circ$ ) with water roll-off direction noted by the dashed arrow. The drop pins on its trailing edge (left side of drop shown with solid arrow) causing the drop to no longer have a circular contact area and to adopt a teardrop-like shape. Also, small drops (circled areas) do not roll off the surface easily.

Pockets of air between the surface roughness and the water drop (Cassie-Baxter model<sup>4</sup> and Figure 20) can also be seen on the three images (specially on c). On a smooth surface, surface refraction through the drop looks smooth. a) Top view. b) Angled view. c) Close-up of pinning point and air pockets visible through the drop.

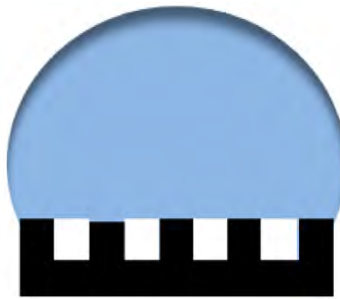


Figure 20: Cassie-Baxter model describes no penetration of the liquid into the surface's roughness (black grooves). The liquid therefore sits on the peaks of the roughness and on the pockets of air (white sections between the black grooves). Drop size and roughness features are not to scale. Usually roughness features are in the order of  $\mu\text{m}$  and  $\text{nm}$  while drops are in the order of  $\text{mm}$  and  $\text{cm}$  (Image and wording used with the kind permission of Parham Zabeti).

It was also noticed that if the surface is sprayed with small drops of water ( $\sim 1 - 3 \text{ mm}$  in diameter) and tilted vertically ( $90^\circ$ ), some of them do not roll off the surface. It might be a combined effect of the creases already present on the surface (from the stomping) as well as from the changes in the surface topography as shown in Figure 21. This amount of water on the surface is more noticeable on the third sample than it is on the first or second samples.



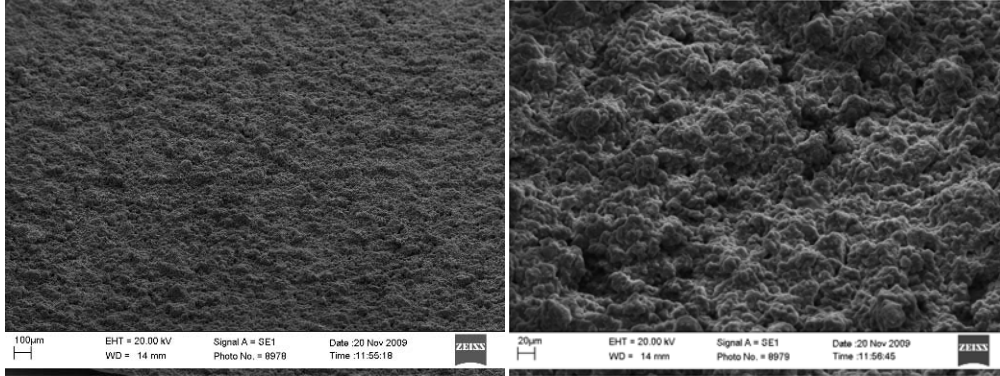
*Figure 21: Small water drops stick to the surface of the third sample when tilted vertically (90°). This shows that the surface has been worn to some extent since this behaviour is not seen on the first or second sample. The drops stick to the surface because of the changes in the topography of the sample's surface and perhaps also because of the creases created (and visible) from when the sample was stomped on.*

### **3.3 RESULTS AND ANALYSIS**

#### **3.3.1 SEM Images**

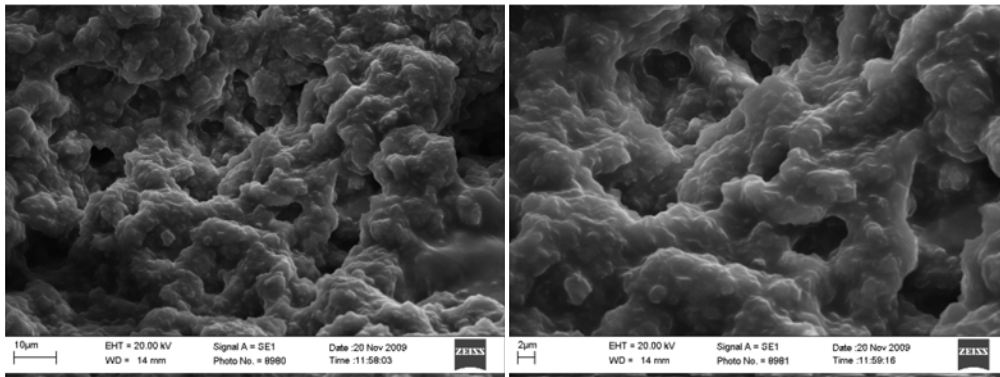
##### **3.3.1.1 First Sample - Unworn:**

The information for studying the roughness of the surface of the first sample (unworn) was gathered using SEM and CSM. It was noted with both methods that there are different roughness scales for this coating as described along the CSM data. Figure 22 shows SEM images of the first sample at different magnifications.



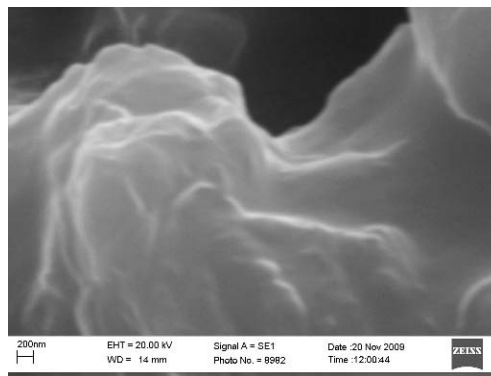
a) 100X. Image Scale is 100  $\mu\text{m}$ .

b) 500X. Image Scale is 20  $\mu\text{m}$ .



c) 2500X. Image Scale is 10  $\mu\text{m}$ .

d) 5000X. Image Scale is 2  $\mu\text{m}$ .



e) 50000X. Image Scale is 2  $\mu\text{m}$ .

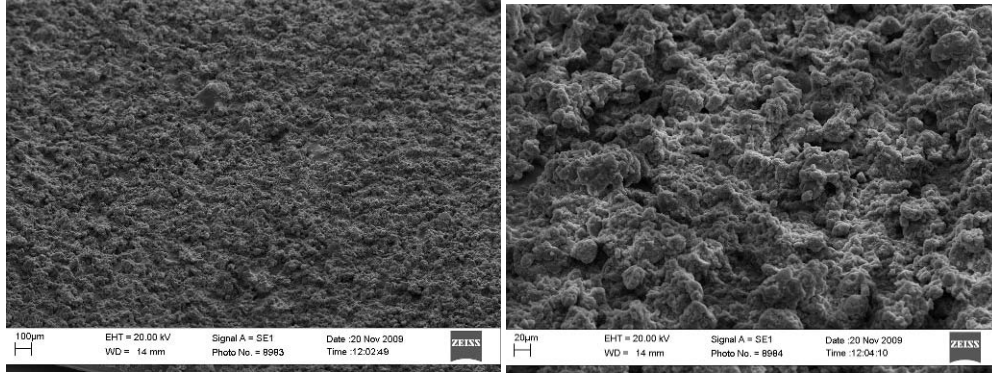
*Figure 22: SEM Images of the first sample (unworn) at 100X, 500X, 2,500X, 5,000X and 50,000X magnification respectively taken at a tilt of 45° showing the detail and different sizes of the roughness features. This sample was coated with the Organoclay Nanocomposite Superhydrophobic Film from the University of Illinois.<sup>9</sup> No details were provided with this sample regarding coating thickness or coating technique.*



The first unworn sample shows a very different surface topography to the Plasma Etched PTFE described in Section 2. It can be clearly seen at magnifications above 500X that the surface's features are not as homogeneous as the peaks seen in the Plasma Etched PTFE. This coating however does have the roughness features (in the order of  $\mu\text{m}$  and  $\text{nm}$ ) required to fulfill Cassie-Baxter model for superhydrophobicity shown in Figure 20. It is also worth noting that there are prominent roughness features at different magnifications, therefore at different scales. This might have an effect on the wetting of the surface as well as on the roughness parameters as described by Ramón-Torregosa.<sup>6</sup> This sample, along with the second and third samples are also analyzed with CSM (later in the report) at different magnifications to show if there is indeed a relationship between the roughness scale and the roughness parameters obtained.

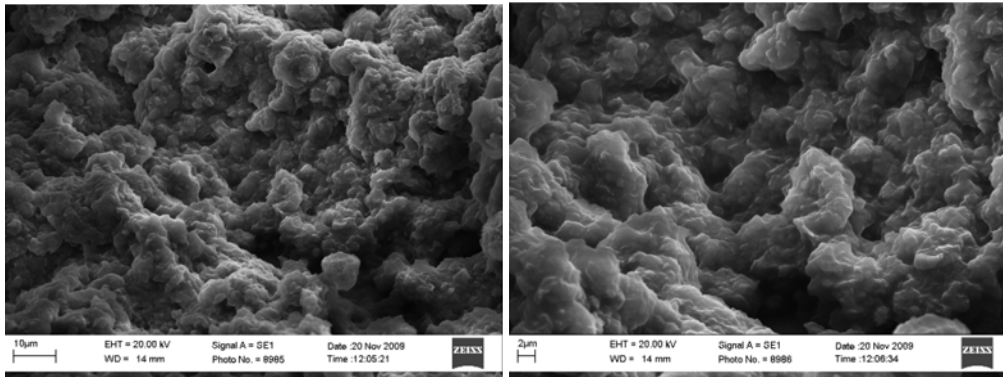
#### **3.3.1.2 Second Sample - Worn by stomping from using as mat:**

Figure 23 shows the second sample (worn by stomping from using as mat) under the SEM for the same magnifications used with the first sample. There appears to be no significant change on the coating and the surface roughness induced by the action of stomping on the surface. Although creases are easily visible on the sample without the use of a microscope as shown in Figure 18c, there is no indication of damage to the coating from the SEM images.



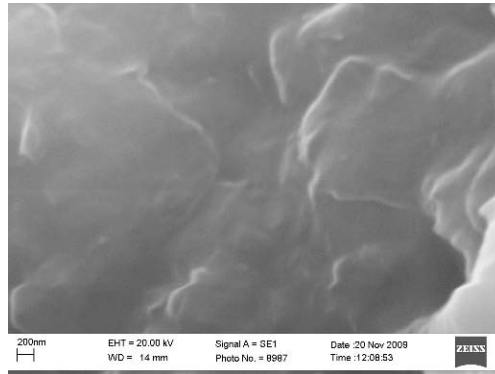
a) 100X. Image scale is 100  $\mu\text{m}$ .

b) 500X. Image scale is 20  $\mu\text{m}$ .



c) 2,500X. Image scale is 10  $\mu\text{m}$ .

d) 5,000X. Image scale is 2  $\mu\text{m}$ .



e) 50,000X. Image scale is 200 nm.

*Figure 23: SEM Images of the second sample (worn by stomping from using as mat) at 100X, 500X, 2,500X, 5,000X and 50,000X magnification respectively taken at a tilt of 45° showing the detail and different sizes of the roughness features. This sample was coated with the Organoclay Nanocomposite Superhydrophobic Film from the University of Illinois.<sup>9</sup> No addition details were provided with this sample regarding coating thickness or coating technique. It was only mentioned that this sample had been stomped on and/or used as a mat*

The SEM images of the second sample shown in Figure 23 show little to no difference to the SEM images obtained from the first sample (unworn) shown in Figure 22. There is an abundance of roughness features that could satisfy the Cassie-Baxter wetting model. The second sample at 100X magnification (Figure 23a) is as homogeneous as the first sample (unworn) at the same magnification (Figure 22a) and shows no damage from stomping.

### **3.3.1.3 Third Sample - Worn by stomping from using as mat + 8 minutes on shaker:**

SEM images for the third sample have not been obtained because that requires damaging the sample to obtain a small piece. Since the amount of samples obtained from the University of Illinois is limited (two samples) and the relationships between wearing, roughness parameters and wetting are still not fully developed, conducting SEM work at this point could stop any additional study on this third sample (i.e. increase wear, collect further roughness data, etc.).

## **3.3.2 CSM Data**

The three samples were analyzed using CSM for gathering all the surface and volume roughness parameters as well as the topography's geometrical features. The data was collected at three different magnifications for each sample: 20X, 50X and 100X. The reasoning being that for the first and second samples, prominent features are visible at the different magnifications used. It is believed that roughness features at different magnifications (scales) would yield different roughness parameters as described by Ramón-Torregrosa<sup>6</sup> in the context of wetting. After collecting all the available roughness parameters defined in Table 1 and looking at the relevant parameters mentioned in Section 1, nine parameters have been identified to generally describe the surfaces' topography: Ra, Rq, Rsk, Rku, Sa, Sq, Ssk, Sku and r.

Since the S parameters are the volumetric counterparts of the linear R parameters, only the S parameter and r (roughness area to projected area ratio) are shown. In theory, for a homogeneous surface, the R and S parameters should match. In this study, the R and the S parameters do match, and are therefore not shown here for simplicity purposes. Figures 24 – 26 show the trends of the selected parameters between the first, second and third sample at different magnifications. The first sample is considered to be the most superhydrophobic, the second sample not as superhydrophobic and the third sample is considered the least superhydrophobic.

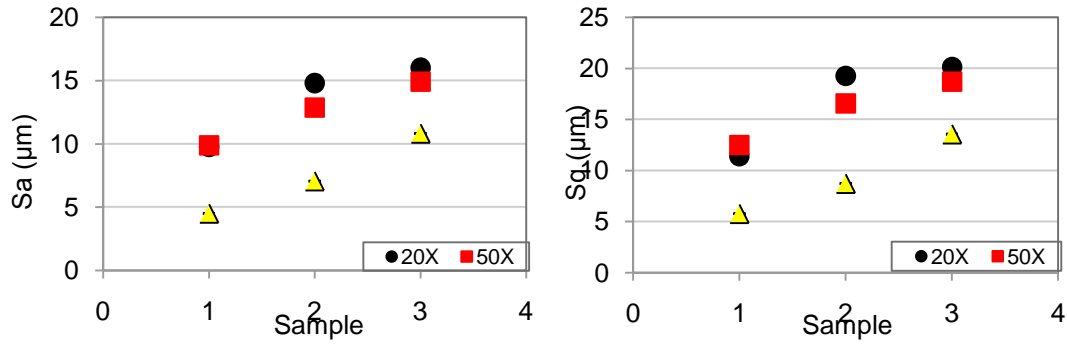


Figure 24: Sa and Sq parameters are the volumetric counterparts of Ra and Rq and are plotted at three different magnifications (20X, 50X and 100X) for the three samples tested. It can be seen that the values for each magnification follow the same trend. However, the 100X magnification data is shifted. This relates to the idea of having more than one roughness scale and its effects on roughness measurements.<sup>6</sup>

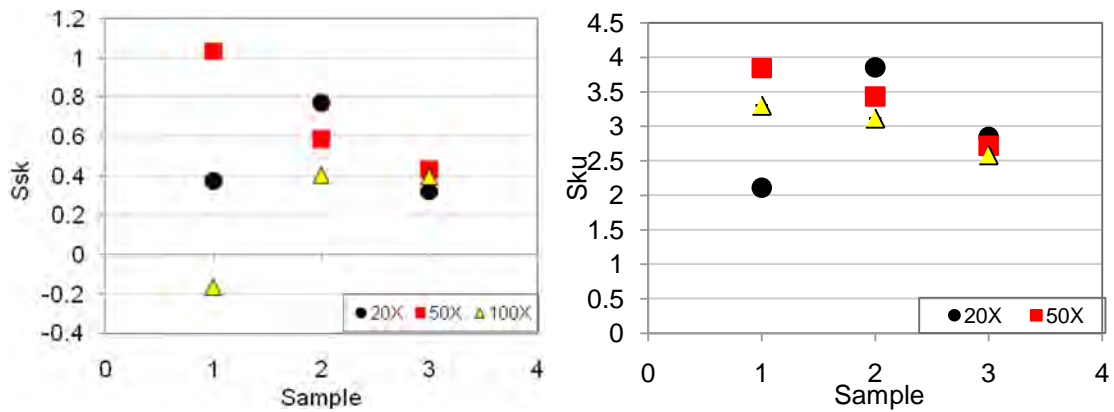


Figure 25: Ssk and Sku parameters are the volumetric counterparts of Rsk and Rku and are plotted at three different magnifications (20X, 50X and 100X) for the three samples tested. It can be seen that the trends for each magnification are very different from each other unlike the plots for Sa and Sq in Figure 24. Ssk and Sku parameters seem to converge at the third sample (the most worn sample), yet the different trends also relate to the idea of having more than one roughness scale.

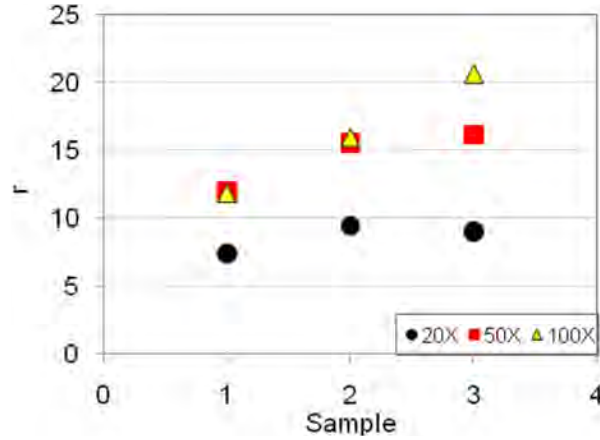


Figure 26: *r* parameter plotted at three different magnifications (20X, 50X and 100X) for the three different samples. The trends for each magnification are similar to the trends of *Sa* and *Sq*. This parameter shows an increasing trend meaning that more surface area has been developed with wear. For this to be possible, either the coatings between samples are different, or, subjecting the surface to wear has modified the original roughness in a way that has increased the distance between the peaks and the valleys.

### 3.4 CONCLUSIONS

The first points to notice from the graphs are the trends of the different magnifications for *Sa* and *Sq* in Figure 24. The data obtained at 20X and 50X is very similar, hinting at the existence of a roughness scale within the resolution of the CSM for such magnifications. The different objectives used (20X, 50X and 100X) have different spatial and vertical resolutions as shown in Table 2. Based on the resolutions used by the 20X and 50X objectives, it can be said that the features of the first roughness scale are approximately larger than 0.449  $\mu\text{m}$  spatially and 0.500  $\mu\text{m}$  vertically for the two objectives to properly capture them.

Table 2: *Spatial and vertical resolutions of CSM objectives used for roughness scale determination*

<i>Objective</i>	<i>Spatial Resolution</i>	<i>Vertical Resolution</i>
<i>20X</i>	0.44979 $\mu\text{m}$	0.500 $\mu\text{m}$
<i>50X</i>	0.18708 $\mu\text{m}$	0.250 $\mu\text{m}$
<i>100X</i>	0.09183 $\mu\text{m}$	0.150 $\mu\text{m}$

On the other hand, the data for *Sa* and *Sq* in Figure 24 at 100X magnification is shifted down  $\sim 6$   $\mu\text{m}$ . This means that the 100X objective is able to capture the second roughness scale with features that range between 0.092  $\mu\text{m}$  and 0.187  $\mu\text{m}$  spatially by 0.150  $\mu\text{m}$  and 0.250  $\mu\text{m}$  vertically. These results show that there might be at least two different and distinct roughness scales on the surfaces since 20X and 50X magnification show similar values but at the same time very different from the 100X magnification. For an ideal surface with only one roughness scale as in micro- or nano-fabricated geometric pillars, the roughness parameters do not show much

variation at different magnifications (to a large extent). Such micro- or nano-fabricated surfaces yield the same Sa and Sq values between different objectives provided that the resolution of each objective is sufficiently small to capture their features (i.e. geometric pillars). This has been verified with test and calibrations runs performed on the CSM (no data collected) with the same samples used and provided by Barnabas.<sup>10</sup>

Although the three samples studied have been worn almost incrementally (based on the samples being progressively less superhydrophobic), the roughness parameters Sa and Sq in Figure 24 and the r parameter in Figure 26 generally show increasing trends under the three magnifications. This increase is indicative of the surface roughening with wear. One idea behind this phenomenon is that the coating is more easily worn off in the portions where it's thinnest, therefore deepening the valleys of the surface. This would change the distance measured between peaks and valleys, effectively making the surface seem as if it is being roughened or as if the peaks are getting taller or the valleys getting deeper. However, nothing conclusive has been established regarding these trends since there is uncertainty between the details of the coating characteristics and technique used from the first to the second sample as well as the wearing method used (stomping vs. abrading) between the second and third sample.

The other two parameters shown in Figure 25, Ssk and Sku, present a trend in which the values seem to converge with increasing wear for the three different magnifications. This would mean that the wear process that these samples have been subject to (stomping and abrading) has made the roughness features more homogeneous, indicating that the samples may have reached a point where they can start wearing evenly. If that is the case, it may explain why the pinning behaviour is first observed for the third sample and not for the second one (or any point in between). In other words, even though the samples have been worn incrementally, while one roughness scale is changed (worn) the other roughness scale might aid in providing superhydrophobicity; or, the combined effect of the different roughness scales and the size of their features might still be significant enough to impact superhydrophobicity favourably.

It is very interesting to note that the parameters shown have different trends between magnifications or roughness scales as described by Ramón-Torregrosa.<sup>6</sup> This variability however, is more apparent in the parameters chosen (Ra, Rq, Rsk, Rku, Sa, Sq, Ssk, Sku and r) and not with all of the parameters available in Table 1. Ideally, parameters like Sa and Sq can be used to establish basic trends regardless of the magnification used or roughness scales available on the sample. On the other hand, parameters like Ssk and Sku and their convergence with incremental wear may be helpful in establishing the transition points in wetting behaviour regardless of the roughness scales.

## 4 Developing Superhydrophobic Coating

---

Considering the results obtained from the samples coated with the superhydrophobic coating from Section 1, it was decided to develop our own version to better understand its properties and to study a wider application range (i.e. glass, paper, wood, textiles, etc.). Also of interest is to study the coating's resistance to wear in relation to the roughness parameters and wetting results as done with the previous samples (Plasma Etched PTFE, aluminum foil coated with superhydrophobic coating and acid etched aluminum) in Section 1 and 2. More precisely, the goals for developing the superhydrophobic coating are:

- To better understand what role the main coating components (i.e. adhesive, nanoclay, Zonyl®) play in the final mix.
- To determine what are the proper coating (i.e. airbrush type, number of coats, etc.) and curing methods (i.e. aerobic, anaerobic, temperature, time, etc.).
- To successfully replicate the level of superhydrophobicity of the samples from Section 1 (aluminum foil coated with superhydrophobic coating) based on the instructions available.
- To investigate the performance of the coating on different materials.
- To further develop the relationship between roughness parameters, surface topography and wetting data.
- To develop a way of making the coating as colorless as possible (samples from Section 1 are yellowish and samples from this section are reddish).

The recipe and instructions used for making the coating used on the samples from Section 2 are provided in the letter 'Transforming Anaerobic Adhesives into Highly Durable and Abrasion Resistant Superhydrophobic Organoclay Nanocomposite Films: A new Hybrid Spray Adhesive for Tough Superhydrophobicity' by Bayer.<sup>9</sup> In this letter, they develop their own bio-adhesive concentration (for roughness), which is then mixed with a fluorinated product (Zonyl® 8740 from DuPont™ for hydrophobicity). This bio-adhesive is the key component in providing the necessary adhesion to different substrates as well as in providing the necessary strength between the coating's components, strengthening its internal structure and making it more resistant to wear. In our own coating solution, we have opted to use a 3M™ Threadlocking Adhesive (Scotch-Weld™ Threadlocker TL62) that provides very similar superhydrophobicity but not as much wear resistance. The idea of using this adhesive came from the documentation of the coating in which they describe using the discontinued 3M™ Scotch-Weld™ 3495 as a substitute to their own bio-adhesive giving them statistically identical wetting results. The purpose of starting with this particular adhesive is mainly for proof of concept and ensuring that similar results can be replicated in our own labs.

So far, three batches of coating have been developed in order to gain understanding on the different properties and components of the coating. Each batch was a different attempt at achieving the results obtained by Bayer; therefore, each batch used different component concentrations in the process of finding the right ratios for achieving superhydrophobicity. The components used and their final concentrations by weight are included in Table 3. This table shows the concentrations of the final and successful Batch # 3.

Table 3: List of components used and their final concentration for making superhydrophobic coating.

<i>Component</i>	<i>Concentration (by weight)</i>
<i>Nanoclay</i>	7 %
<i>DMSO</i>	8.5 %
<i>Adhesive</i>	4 %
<i>Ethanol</i>	30.5 %
<i>Zonyl® 8740</i>	50 %
<b>TOTAL</b>	<b>100%</b>

## 4.1 EXPERIMENTAL DETAILS

### 4.1.1 BATCH # 1

The first batch of coating was made only with 50% of the total mix by weight: The dispersion of Nanoclay in DMSO and adhesive, together diluted in ethanol. This batch was used to coat three samples in order to study surface roughness, effects of coat thickness and proper curing methods. The three samples were treated as follows:

1. Aluminum foil: Applied heavy coat with internal mixing airbrush. Set/cured coating anaerobically (in vacuum oven) overnight at room temperature following the curing instructions for the adhesive.
2. Copper Tape: Applied light coat with internal mixing airbrush. Set/cured coating anaerobically (in vacuum oven) for 30 minutes following the instructions on the letter from the University of Illinois for copper (catalytically active).
3. Aluminum foil: Applied light coat with internal mixing airbrush. Set/cured coating aerobically at 80°C following the instructions on letter from University of Illinois for aluminum (catalytically inactive).

These three samples have also been coated with Teflon® (only half of the sample) in an effort add a fluorinated compound to try to simulate the final result obtained when adding the Zonyl® product originally used in their recipe. This was also done under the assumption that Zonyl® does not contribute to the roughness in the coating; therefore, lightly coating the samples with Teflon™ should be initially similar to what it would be when using Zonyl®. After coating with Teflon™ the three samples exhibit different hydrophobic behaviour and are described as follows:

- Sample 1 (aluminum foil, heavy coat): the most fragile of the three samples. The coat is thicker than the rest and after setting/curing it developed cracks everywhere making it very flaky (probably an exaggerated result of what was published in the letter<sup>9</sup> before adding Zonyl®). Sample was somewhat hydrophobic.
- Sample 2 (copper tape, light coat): copper was used because of the ability of the coating/adhesive to better set/cure on a more catalytically active surface. It is still fragile



(coating can be easily smudged off) but the most hydrophobic of the samples after coating with Teflon®.

- Sample 3 (aluminum foil, thin coat): the most robust of the three (coating is more resistant to smudging than on copper tape) yet the least hydrophobic after coating with Teflon®.

No wetting tests were conducted on these samples with ADSA. However, based on wetting observations, the static contact angles are approximately as follows:

- Sample 1: ~120° - 140° (hydrophobic)
- Sample 2: ~140° - 150° (almost superhydrophobic)
- Sample 3: ~90° - 120° (barely hydrophobic)

So far it has been established that having the proper coating thickness and curing the samples properly are of high importance. On an initial understanding, thick coats would render them too fragile (easily smudged off or developing cracks as with sample 1). Also, it was seen that three different 'appropriate' methods following three different instructions for curing the adhesive yielded three very different results. Figure 27 shows SEM images of the three different samples without the Teflon™ coating.

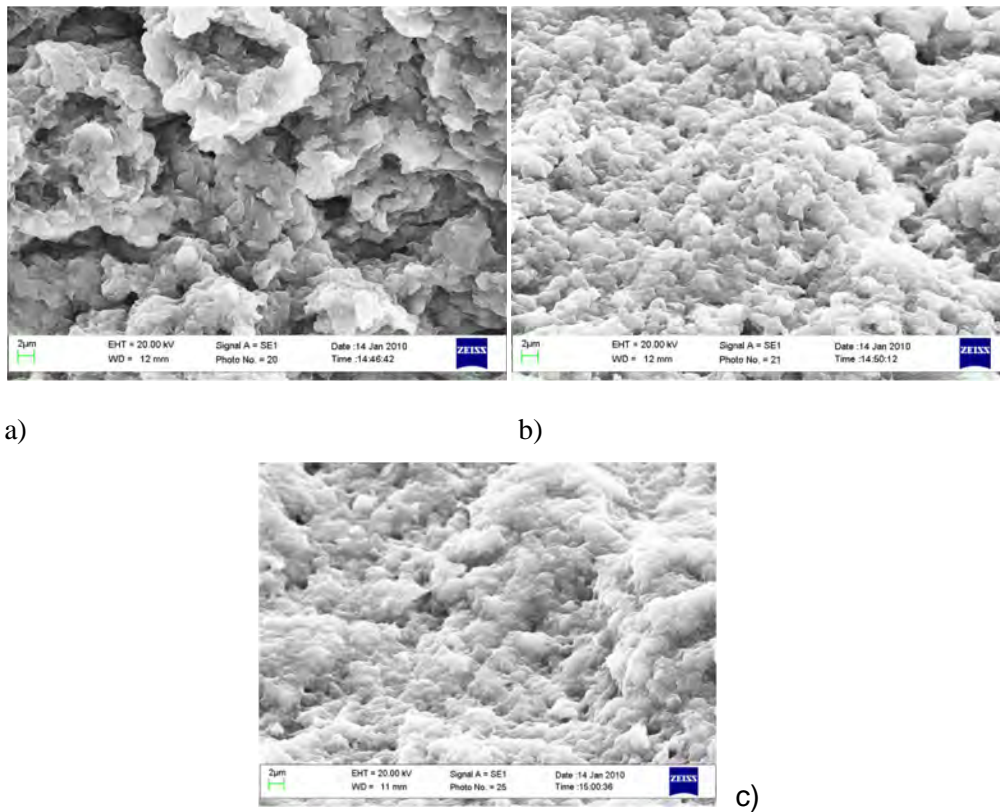


*Figure 27: 5,000X SEM Images of one coat of the first batch of superhydrophobic coating without additional Teflon™ coating (scale is 2 μm for the three images). It can be seen that this mix (without Zonyl®) seems to provide the required surface roughness to satisfy the Cassie-Baxter wetting model. However, a significant difference can be observed between the sizes of the*

*roughness features in the three samples, with sample 1 having the roughest appearance. a) Heavy coat on aluminum foil. b) Light coat on copper tape. c) Light coat on aluminum foil.*

This first batch, although almost superhydrophobic in the best case (sample 2: thin coat on copper tape), is still far from exhibiting the wetting behaviour observed on the samples sent from the University of Illinois (see Section 2). Although the use of a different adhesive would certainly play a role (mainly in the durability of the coating), it is the lack of the fluorinated compound in the mix (Zonyl® 8740) that is making the difference in the wetting behaviour observed. It has also been determined that coating the samples with Teflon is not sufficient to make the samples superhydrophobic. The effect of a fluorinated coating is not as powerful as having it being part of the mix, bonding with the other components.

#### 4.1.2 BATCH # 2

The second batch of coating was developed according to the instructions in the letter, although this time including the fluorinated product, Zonyl® 8740. For this batch of coating, three samples were coated three times, each sample coated with a different thickness by using the internal mixing airbrush. Sample 1 was coated with three light coats, Sample 2 was coated with three medium coats and Sample 3 was coated with three heavy coats. This was done in order to study the effect of different thicknesses on superhydrophobic performance. Figures 28 – 30 are SEM images that show the three different samples coated and the different thicknesses achieved on them with the second batch of coating.

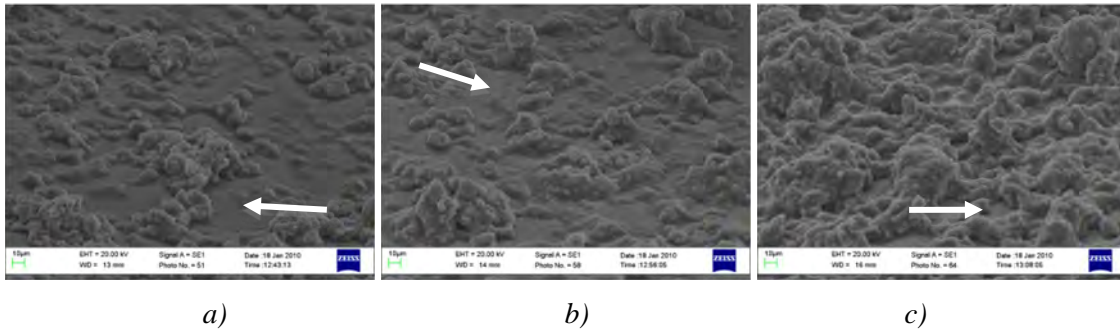


*Figure 28: 1,000X SEM images taken at 45° of the second batch of coating applied in light coats on Sample 1 (scale is 10 µm for the three images). It can be seen that there are portions of aluminum foil that were not covered (areas denoted by white arrows). It can also be observed that the roughness of the coatings is very different with Zonyl® incorporated in the mixture. The roughness features do not look as jagged and sharp as they did in Figure 27. a) 1 Coat. b) 2 Coats. c) 3 Coats.*

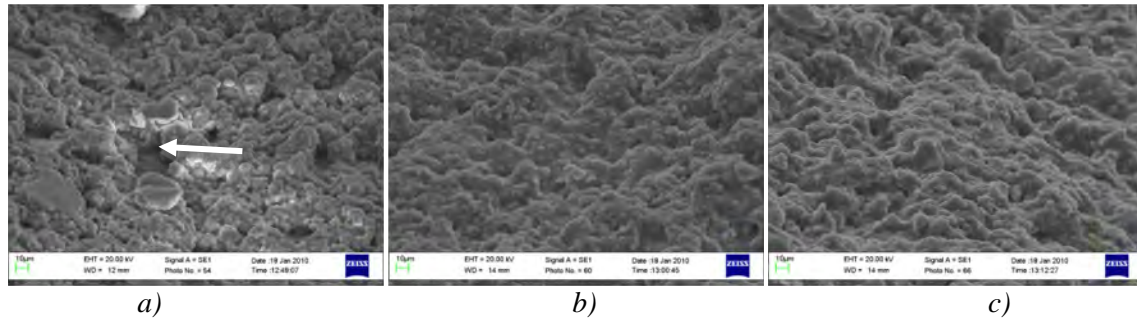


*Figure 29: 1,000X SEM images taken at 45° of the second batch of coating applied in medium coats on Sample 2 (scale is 10 μm for the three images). There are still portions of aluminum foil that were not covered (areas denoted by white arrows) with the first coat. Coating is apparently more even than with the thinner coats from Figure 28. a) 1 Coat. b) 2 Coats. c) 3 Coats.*

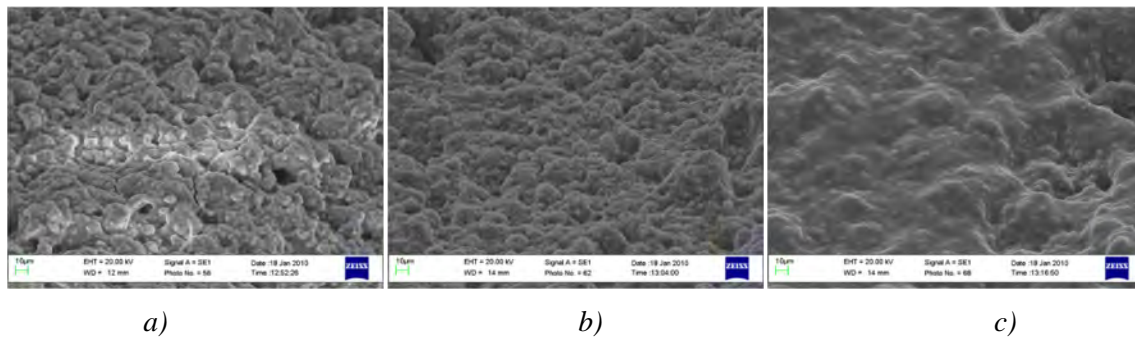


*Figure 30: 1,000X SEM images taken at 45° of the second batch of coating applied in heavy coats on Sample 3 (scale is 10 μm for the three images). There are no portions of aluminum foil that were not covered. The coating appears more even than those on Samples 1 and 2. After three coats (c), roughness features are not as prominent as on other samples. a) 1 Coat. b) 2 Coats. c) 3 Coats.*

The samples were cured in the oven at 80°C for three hours as described in the instructions. Although no wetting tests were conducted using ADSA, on wetting behaviour observations, the samples show improved results over the first batch of coating. The samples are hydrophobic overall, with some small portions that behave superhydrophobically as samples obtained and described in Section 3. Particularly, Sample 2 (medium coat thickness) appeared to be the most hydrophobic of the three after three coats based on wetting observations.

Even though the procedure was performed as indicated in the instructions from the letter, the results obtained were not what were expected. None of the nine different coatings used yielded similar wetting behaviour as what was observed with the original recipe of the coating, even after allowing the samples to cure properly. Although the only difference between the original recipe and our own version of it was the adhesive used, it was not expected to make a big difference in the wetting behaviour since it was shown<sup>9</sup> that the threadlocking adhesive provided statistically equal results. It was therefore necessary to look again at the recipe to verify that the different

component ratios and concentrations were used correctly. This new revised batch of coating is Batch # 3.

### **4.1.3 BATCH # 3**

When making the third batch of coating, a slightly different interpretation was given to the recipe provided in the letter documenting the superhydrophobic coating. The difference in interpretation arose from whether to use concentrations as g/mL of solvent or g/mL of solution, both of which are valid concentration nomenclatures, yet not clearly stated in the letter. The new interpretation (g/mL of solution) reduced the amount of DMSO by ~75% while increasing the amount of Ethanol by ~100% to keep the concentrations consistent. The final concentrations achieved are mentioned at the beginning of this section and are included in Table 3.

With this new batch and with it a higher amount of Ethanol, it was determined that the coating would be less viscous, allowing for a better spray pattern when using the internal mixing airbrush as described in the letter. However, using an external mixing airbrush has also been considered but has not been used yet because of its thicker and coarser spray. To start, three samples were coated once with different thicknesses (light, medium and heavy). The initial observations from the three samples are as follows:

#### Sample 1

- Light coat.
- Sample is hydrophobic with superhydrophobic portions (much more hydrophobic than those from Batches 1 and 2).

#### Sample 2

- Medium coat.
- Sample is also hydrophobic with superhydrophobic portions (much more hydrophobic than those from batches 1 and 2).
- Slightly more hydrophobic than Sample 1.

#### Sample 3

- Heavy coat.
- Sample is superhydrophobic as expected.
- Seems to be as superhydrophobic as the samples obtained from the University of Illinois.
- There are a couple of spots on the sample where the coating seems to be thicker; however, this spots are not superhydrophobic and seem to be very sticky. Might relate to Figure 30c.

These samples have also cured in the oven for 3 hours at 80°C. However, after letting the samples sit at room temperature overnight, they seem to have become slightly more superhydrophobic. This would mean that the curing time and/or temperature could be increased. Consideration needs to be also given to better controlling the transitions in temperature (from room temperature to curing and vice versa).

From the success of this batch of coating, it was decided to use it on different substrates to determine if the coating would adhere and cure properly on other materials with smooth or rough surfaces. The coating was used to spray one medium thickness coat on aluminum sheet, glass, copper tape, cardboard and wood. These samples were also allowed to cure for 3 hours at 80°C. Upon curing, the samples were allowed to cool for 30 minutes at room temperature. After curing, wetting observations were carried out on the samples and they all showed excellent and impressive superhydrophobic behaviour (with only one coat of the coating). Interestingly, the smoother materials (aluminum sheet, glass and copper tape) appear to be slightly less superhydrophobic. This indicates that the coating is benefiting from the already present roughness found on the cardboard and balsa wood.

Achieving successful results on cardboard, glass and wood shows that the coating is capable of adhering and curing properly in different materials with different surface chemistry and roughness. This opens the doors to exploring the application of coatings on different objects and materials to make them superhydrophobic. Figures 31 – 34 show SEM images at 1,000X magnification of the third batch of superhydrophobic coating on aluminum foil, glass, cardboard and balsa wood respectively.

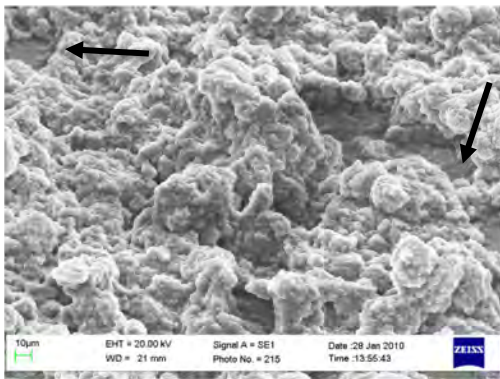


*Figure 31: 1,000X SEM Image of 1 coat of Batch # 3 of Superhydrophobic Coating on Aluminum foil. Coating and roughness features appear very similar to those on the samples obtained from the University of Illinois (Figure 22). Some portions of uncoated aluminum foil can be seen (area denoted by black arrow). Image scale is 10 µm.*

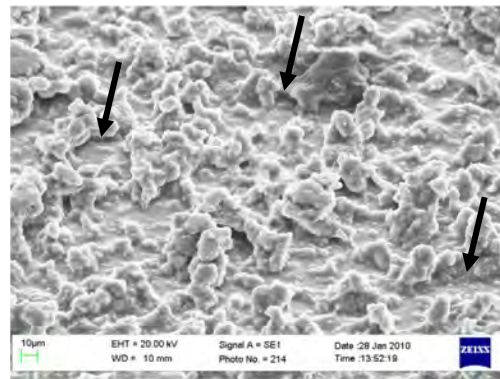


*Figure 32: 1,000X SEM Image of 1 coat of Batch # 3 of Superhydrophobic Coating on Smooth Glass. Sample is slightly less superhydrophobic than the other samples. Might be because some more areas of the glass surface were not coated (areas denoted by white arrows). Image scale is 10 µm.*



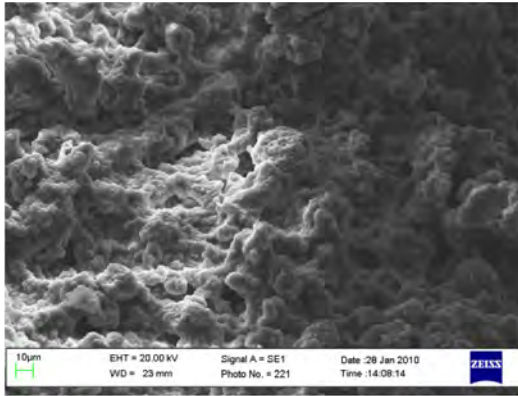


*Figure 33: 1,000X SEM Image of 1 coat of Batch # 3 of Superhydrophobic Coating on Cardboard. The surface of the cardboard is not visible, indicating that either the coat was properly applied or the roughness of the cardboard surface has features similar in size to those added with the coating. This may explain why coated cardboard appears to be even more superhydrophobic than coated glass (Figure 32). Image scale is 10 µm.*

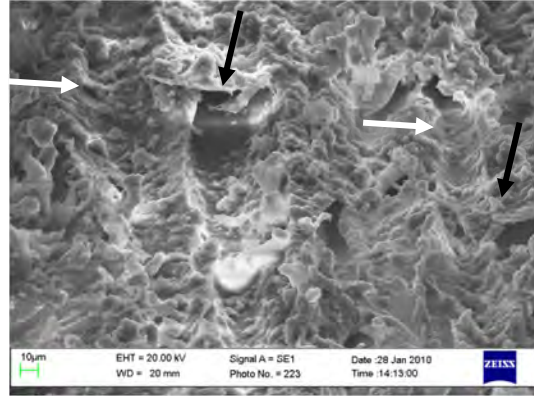


*Figure 34: 1,000X SEM Image of 1 coat of Batch # 3 of Superhydrophobic Coating on balsa wood. This surface is also very superhydrophobic. This may be in part due to the roughness already present on the wood before coating (similar to the cardboard case in Figure 33). This image shows that some portions of the surface were not coated (denoted with black arrows), but it also shows how the coating has been moulded to fit the shape of the roughness features already present (white arrows). Image scale is 10 µm.*

## 4.2 RESULTS AND ANALYSIS

Although the previous samples coated with the third batch of coating show excellent superhydrophobic behaviour, there are still a few factors in the process that have not been determined. It is not clear yet, which exactly are the most adequate coating and curing methods. It is evident from the data gathered with the three batches that there is a significant difference between the different coat thicknesses (Figures 28 – 30). It has also been determined that curing the samples for 3 hours at 80°C is sufficient; however, it has also been found that the samples still cure for a period of several hours following the curing performed in the oven (slightly impacting the wetting behaviour). Also, the data collected thus far is purely qualitative. Surface roughness parameters and contact angles need to be measured accordingly.

The first factor to investigate is coating technique (i.e. airbrush type, coat thickness, number of coats, etc.). For this part of the experiment, eight aluminum sheet samples were prepared. Samples 1 - 4 were incrementally coated with an external mixing airbrush (coarser spray pattern, better for viscous coatings, better for large areas) while samples 5 - 8 were incrementally coated only with the internal mixing airbrush. After coating samples 1 - 4 with the external mixing airbrush, it was found that the samples were not completely superhydrophobic and were coated up to two more times with the internal mixing airbrush. The coating type, number of coats, total coating thickness and wetting data for each sample are shown in Table 4. Wetting data for these samples is plotted in Figure 35.

Table 4: Number and type of coating applied to aluminum sheet samples along with coat thickness, advancing, receding contact angles and contact angle hysteresis.

Sample	EM Coats	IM Coats	Total Coats	Total coat thickness ( $\mu\text{m}$ )	Advancing (degrees)	Receding (degrees)	Hysteresis (degrees)
1	1	1	2	8.68	159.92	150.60	9.32
2	1	2	3	6.77	167.01	158.94	8.06
3	2	2	3	24.13	173.34	155.57	17.76
4	3	2	5	34.93	166.72	149.02	17.70
5		2	2	14.61	168.46	153.67	14.79
6		2	2	16.09	171.05	148.64	22.40
7		3	3	12.28	168.72	155.03	13.69
8		4	4	17.15	172.19	165.33	6.85

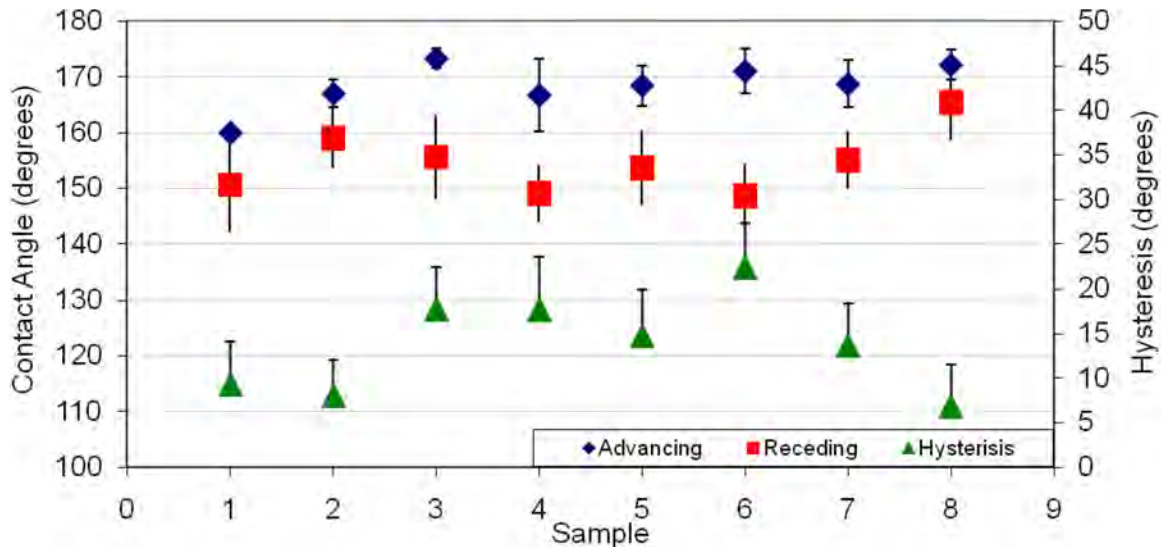


Figure 35: Advancing, Receding (left axis) and Hysteresis (right axis) contact angles of water for each of the coated aluminum sheet samples. Although all the surfaces are superhydrophobic, it can be seen that the samples coated with the external mixing airbrush (1 - 4) benefit from additional coats. The samples coated with the internal mixing airbrush (5 - 8) show very little change in the advancing contact angle with increased number of coats yet show an improvement in the receding contact angle.

It has been determined from the data in Table 4 and Figure 35 in the context of wetting that the most efficient results were achieved by coating the samples with the internal mixing airbrush. It was initially thought at the beginning of the testing with these samples, that coating the samples with the external mixing airbrush first would be beneficial. The idea was that the external mixing airbrush would provide a basic coat that would already be hydrophobic (because of Zonyl®), therefore, any uneven distribution of an additional coating (i.e. internal mixing airbrush spray pattern as seen on Figure 32 for smooth glass) would still render the surface superhydrophobic. Based on Table 4 and Figure 35, it is clear that the benefit of having that basic coat from the external mixing airbrush is outweighed by using less coating with the internal mixing airbrush (i.e. less coats) while still achieving higher advancing contact angles.

Also worth noting is that the eight samples described with Table 4 and Figure 35 were modified for the wetting tests (drilled a hole through them for the discharge syringe with water to go through) after the samples were coated. In other words, the samples were drilled through the coating. This may have altered or damaged the coating on the area immediately surrounding the drilled hole. There is no way of determining whether having drilled this hole had an effect on any of the wetting measurements taken.

For this reason, four new samples were made, drilled for the wetting tests and subsequently coated incrementally with the internal mixing airbrush. Wetting tests were performed and coating thickness measurements were taken on these samples. Table 5 includes coating information, wetting data and coating thickness. Figure 36 shows the wetting data for this set of four samples.

Table 5: Number of coats applied to aluminum sheet samples along with coat thickness, advancing, receding contact angles and contact angle hysteresis.

Sample	IM Coats	Total coat thickness ( $\mu\text{m}$ )	Advancing (degrees)	Receding (degrees)	Hysteresis (degrees)
1	1	11.01	170.11	154.73	15.37
2	2	17.14	170.42	155.79	14.62
3	3	27.94	172.98	156.67	16.31
4	4	30.05	172.63	160.05	12.57

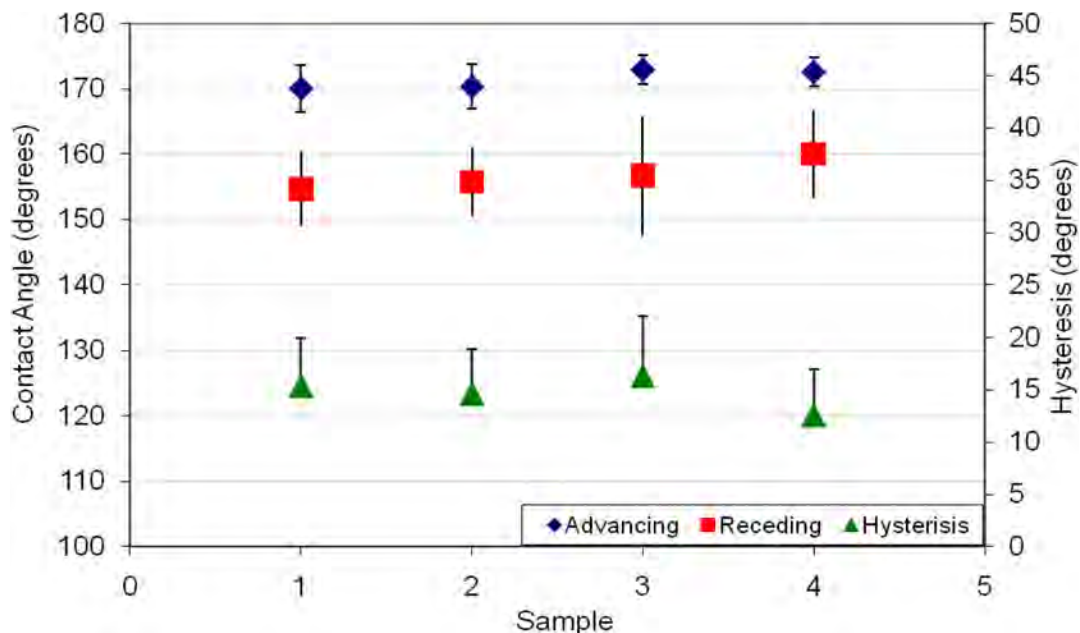


Figure 36: Advancing, Receding (left axis) and Hysteresis (right axis) contact angles of water for each of the coated aluminum sheet samples. These samples are coated incrementally only with the internal mixing airbrush. There is a very slight increasing trend for the advancing and receding contact angles with increased number of coats. There is also a very slight decrease in hysteresis for the same incremental coating.

The data shown on Table 5 and Figure 36 shows the benefit of additional coatings from a wetting perspective. However, the increases in both advancing and receding contact angles are very



small. Hysteresis also sees a decrease with increments in number of coats on a sample, but at the same time is a very small decrease. No CSM data has been gathered for these samples yet. Such roughness parameter data may provide further clues into what is changing on the sample's surface to make them better with increased coatings. No wear tests have been conducted on these samples either. It is unknown what the benefit of having multiple coatings is in the context of wearing and durability.

## 5 CONCLUSIONS AND FUTURE WORK

---

The superhydrophobic coating developed by Bayer<sup>9</sup> has been successfully replicated and allowed us to obtain very similar superhydrophobic properties and wetting behaviour to that observed on the samples provided by the University of Illinois (Section 3). It is believed however that the main purpose of the bio-adhesive developed by them is to provide strength to the coating, making it more resistant to wear. It has been also been determined that curing and coating methods are crucial for obtaining adequate results. The samples studied showed better results when curing aerobically at a temperature of 80°C for 3 hours and when coated incrementally with an internal mixing airbrush.

Collecting roughness parameter data will be done next on the superhydrophobic samples. From this data, better connections will be made between the surface topography shown in the SEM images, the coating methods as well as the wetting data obtained. Although some of the parameters have been selected to be the best descriptors of surface properties, all the parameters will be taken into account. The idea of roughness scales explained in Section 1 will be revisited now that there is more control over how the coating is sprayed onto the various surfaces.

It is also necessary to conduct wear tests on the samples coated with our superhydrophobic coating in order to determine its wear resistance. Now that the recipe for the coating has been successfully replicated, different adhesives may be used in order to achieve different properties. The goal is to find an adhesive that makes these surfaces very robust and resistant to different types of wear (i.e. abrasive, impact, scratching, etc.) while making it practical for diverse applications. The first step in this direction has already been taken and a clear threadlocking adhesive with similar properties has been used with success in the beginning of the year 2 activities. This adhesive would allow the coating to be almost colorless, making the coating more desirable for applications where added color is not wanted.

Currently, other materials have been coated with the superhydrophobic coating: paper, cotton, polyester/nylon, fine metallic mesh and composite materials. These samples show good superhydrophobic behaviour so far. However, no further testing has been done. These were coated as part of an attempt to determine how versatile this coating is. However, a more systematic approach for these unconventional surfaces will be undertaken in future work.

## References

---

- [1] T. Young, "An Essay on the Cohesion of Fluids," *Philosophical Transactions*, no. 95, pp. 65-87, 1805.
- [2] S. Wang and L. Jiang, "Definition of Superhydrophobic States," *Advanced Materials*, vol. 19, no. 21, pp. 3423-3424, Oct. 2007.
- [3] C. Extrand, "Self-Cleaning Surfaces: An Industrial Perspective," *MRS Bulletin*, p. 733, 2008.
- [4] A.B.D Cassie and S. Baxter, "Wettability of Porous Surfaces," *Trans. Faraday Soc.*, vol. 40, pp. 546-551, 1944.
- [5] J. Ng, "Summary of Wear Test on Superhydrophobic Surfaces from 01/05/09 - 01/09/2009," Mechanical Engineering, Univeristy of Alberta, Edmonton, Final Report 2009.
- [6] P. J. Ramón-Torregrosa, M. A. Rodríguez-Valverde, A. Amirfazli, and M. A. Cabrerizo-Vílchez, "Factors affecting the measurement of roughness factor of surfaces and its implications for wetting studies," *Colloids and Surfaces A: Physicochemical and Engineering Aspects*, vol. 323, no. 1-3, pp. 83-93, June 2008.
- [7] R. N. Wenzel, "Resistance of solid surfaces to wetting by water," *Industrial and Engineering Chemistry*, vol. 28, no. 8, pp. 988-994, August 1936.
- [8] D. Barona, "Studying the Wear of Superhydrophobic Surfaces: Superhydrophobic Plasma Etched Teflon," Department of Mechanical Engineering, University of Alberta, Edmonton, Progress Report 2009.
- [9] I. S. Bayer, A. Brown, A. Steele, and E. Loth, "Transforming Anaerobic Adhesives into Highly Durable and Abrasion Resistant Superhydrophobic Organoclay Nanocomposite Films: A New Hybrid Spray Adhesive for Tough Superhydrophobicity," *Applied Physics Express*, vol. 2, p. 125003, 2009.
- [10] Barnabas, "Surfaces of Different Pillar Shapes," Department of Mechanical Engineering, University of Alberta, Edmonton, Progress 2008.
- [11] P. L. Menezes, Kishore, and S. V. Kailas, "Effect of surface roughness parameters and surface texture on friction and transfer layer formation in tin-steel tribo-system," *Journal of Materials Processing Technology*, vol. 208, pp. 372-382, 2008.

This page intentionally left blank.

## **Annex A    Cleaning Procedure for Samples Worn in Shaker**

---

Clean sample in 100% ethanol in ultrasonic bath for 15 minutes

- Fill a 150mL beaker to the 40mL mark with 100% ethanol and place it inside the ultrasonic cleaner.
- Fill the ultrasonic cleaner with water so that the level of water reaches the 60mL mark on the beaker.
- Place sample in beaker.
- Let it clean for 15 minutes.
- Remove sample from beaker.
- Rinse sample with ethanol or DI water.
- Let sample air-dry.
- Dispose of ethanol as 'Used Ethanol'.
- Rinse beaker with DI water, ethanol or acetone.
- Let it air-dry.
- Cover ethanol beaker with aluminum foil to minimize contamination of beaker.

Make note of any previous wear marks and/or imperfections on the surface or the material before continuing with characterization or additional wear.

This page intentionally left blank.

## **Annex B Procedure for Wearing Superhydrophobic Samples Abrasively with Shaker**

---

### **PREPARATIONS**

#### **SHAKER**

- Measure volume and weight of glass beads (or abrading material) before starting.
- Inspect glass beads (or abrading material) for foreign material and or particles that contaminate it.
- Ensure that the shaker is running appropriately.
  - ◆ Check belt tension and bearing lubrication.
  - ◆ Check nuts and bolts and make sure they are properly tightened.
- Shaker must be placed on a solid and stable surface.

#### **SAMPLE**

- Ensure that the sample is the same size as the insert in the pan.
- Ensure that the sample sits flush inside the pan.
  - ◆ Very important for the sample not to sit too low or too high.
- Make sure the sample is clean
  - ◆ Clean following procedure on Appendix A

### **WEAR TESTING THE SAMPLE**

#### **CYCLE**

- Clean
- Wear
- Wetting Test/CSM
- Wear
- Clean
- Wetting Test/CSM
- Wear
- etc.

## WEARING

- Remove abrading material from shaker so that it doesn't interfere with the insert in the shaker and or with placing the sample in the insert
- Follow the above preparations
- Place double sided tape in the insert inside the shaker where the sample goes
- Place the sample on top of the double sided tape
  - ◆ Fix sample properly by only touching edges that are not to be considered under wetting tests
- Carefully pour sand back inside the shaker by avoiding creating extra damage on the surface of the sample
- Wear the sample at desired speed and interval
- Remove abrading material surrounding the sample without touching the sample and/or the material right above the sample
- Once sample is clear, remove sample very carefully
- Blast sample with air or nitrogen to remove glass beads still present on the surface
- Place sample in cleaning beaker for cleaning following the procedure described in Appendix A.
- Let sample air dry

## WETTING TEST

- Use double sided tape on the back of the sample
- Affix sample on aluminum sample holder
- *Ensure that the sample lays completely flat and remove any excess tape that may interfere with ADSA*
- Place sample on Contact Angle Machine and conduct wetting tests following the standard procedure for operating ADSA
  - ◆ Ensure that the drop behaves reasonably as expected under manual control conditions
- Run test with following parameters
  - ◆ ADVANCING
    - Imaging interval: 1000 ms
    - Initial Volume: 20  $\mu$ L



- Final Volume: 60  $\mu\text{L}$
- Speed/Rate: 0.5  $\mu\text{L/s}$
- ◆ RECEDING
  - Initial Volume: 60  $\mu\text{L}$  (obtained automatically from advancing conditions)
  - Final Volume: 0  $\mu\text{L}$
  - Speed/Rate: 0.5  $\mu\text{L/s}$  (obtained automatically from advancing conditions)
- ◆ ANALYSIS/MEASUREMENTS
  - Conduct analysis/measurements as instructed on operating ADSA
- ◆ Continue conducting wear on sample as desired

This page intentionally left blank.

## Annex C Drop Weight Wear Testing Procedure

---

### PREPARATIONS

#### RIG

- Calibrate drop height by measuring the distance between the marks on the guide cylinder and the top of the block placed on the sample
- Inspect for proper vertical alignment of the guide cylinder to ensure that there would be none to minimal contact between the dropping weight and the inner walls of the cylinder
- Ensure that the whole rig is securely resting on the floor away from other equipment should it tip over and fall.
- Make sure the different parts are and feel secure and solid
- Check nuts and bolts and make sure they are properly tightened
- Characterize the side of the acrylic block that would contact the sample upon impact.

#### SAMPLE

- Make sure the sample is clean
  - ◆ Clean following procedure on Appendix A.
- Characterize surface with CSM before wearing

#### WEAR TESTING THE SAMPLE

#### CYCLE

- Clean
- Wear
- Wetting Test/CSM
- Wear
- Clean
- Wetting Test/CSM
- Wear
- etc.

#### WEARING

- Ensure that the sample rests on a clean surface

- Ensure that the block that rests on top of the surface (to distribute the impact uniformly over the entire surface) is clean and smooth.
- Follow the above preparations
- Place double sided tape on the portion of the surface where the sample would rest
- Place the sample on top of the double sided tape
  - ◆ Fix sample properly by only touching edges that are not to be considered under wetting tests
- Carefully place acrylic block on top of the sample by avoiding creating extra damage on the surface of the sample
- Drop the weight from the desired height
- After impact, remove weight first by pulling on the string attached.
- Once weight is removed from the cylinder, remove the acrylic block from resting on the sample
- Once sample is clear, remove sample very carefully
- Blast sample with air or nitrogen to remove any foreign material present on the surface of the sample
- Place sample in cleaning beaker for cleaning following the procedure described in Appendix A.
- Let sample air dry

#### WETTING TEST

- Follow the same wetting test procedure described in Appendix B.

## **List of symbols/abbreviations/acronyms/initialisms**

---

Refer to Table 1 for list of roughness parameters

ADSA	Axisymmetric Drop Shape Analysis
CSM	Confocal Scanning Microscope
DND	Department of National Defence
DRDC	Defence Research & Development Canada
DRDKIM	Director Research and Development Knowledge and Information Management
R&D	Research & Development
SEM	Scanning Electron Microscope
SHS	Superhydrophobic Surface

This page intentionally left blank.

## Distribution list

---

Document No.: DRDC Atlantic CR 2010-315

### **LIST PART 1: Internal Distribution by Centre**

- 3 DRDC Atlantic Library
- 1 Paul Saville, DRDC Atlantic
- 1 Calvin Hyatt, DRDC Atlantic

---

5 TOTAL LIST PART 1

### **LIST PART 2: External Distribution by DRDKIM**

- 1 Library and Archives Canada, Attn: Military Archivist, Government Records Branch
- 1 DRDKIM
- 1 Scott Duncan, DRDC Suffield
- 1 Dr Amirfazli, Department Mechanical Engineering, University of Alberta, Edmonton, Alberta, T6G 2G8

---

4 TOTAL LIST PART 2

**9 TOTAL COPIES REQUIRED**

This page intentionally left blank.



**DOCUMENT CONTROL DATA**

(Security classification of title, body of abstract and indexing annotation must be entered when the overall document is classified)

1. ORIGINATOR (The name and address of the organization preparing the document. Organizations for whom the document was prepared, e.g. Centre sponsoring a contractor's report, or tasking agency, are entered in section 8.)  Alidad Amirfazli Department of Mechanical Engineering University of Alberta Edmonton, Alberta, T6G 2G8		2. SECURITY CLASSIFICATION (Overall security classification of the document including special warning terms if applicable.)  UNCLASSIFIED	
3. TITLE (The complete document title as indicated on the title page. Its classification should be indicated by the appropriate abbreviation (S, C or U) in parentheses after the title.)  Superomniphobic Surfaces for Military Applications: Nano- and Micro-Fabrication Methods: Chapter 2: Investigation of Wear for Superhydrophobic Surfaces and Development of New Coatings			
4. AUTHORS (last name, followed by initials – ranks, titles, etc. not to be used)  Amirfazli, A.			
5. DATE OF PUBLICATION (Month and year of publication of document.)  January 2011		6a. NO. OF PAGES (Total containing information, including Annexes, Appendices, etc.)  72	6b. NO. OF REFS (Total cited in document.)  11
7. DESCRIPTIVE NOTES (The category of the document, e.g. technical report, technical note or memorandum. If appropriate, enter the type of report, e.g. interim, progress, summary, annual or final. Give the inclusive dates when a specific reporting period is covered.)  Contract Report			
8. SPONSORING ACTIVITY (The name of the department project office or laboratory sponsoring the research and development – include address.)  Defence R&D Canada – Atlantic 9 Grove Street P.O. Box 1012 Dartmouth, Nova Scotia B2Y 3Z7			
9a. PROJECT OR GRANT NO. (If appropriate, the applicable research and development project or grant number under which the document was written. Please specify whether project or grant.)  12SZ20		9b. CONTRACT NO. (If appropriate, the applicable number under which the document was written.)  W7707-098197	
10a. ORIGINATOR'S DOCUMENT NUMBER (The official document number by which the document is identified by the originating activity. This number must be unique to this document.)		10b. OTHER DOCUMENT NO(s). (Any other numbers which may be assigned this document either by the originator or by the sponsor.)  DRDC Atlantic CR 2010-315	
11. DOCUMENT AVAILABILITY (Any limitations on further dissemination of the document, other than those imposed by security classification.)  Unlimited			
12. DOCUMENT ANNOUNCEMENT (Any limitation to the bibliographic announcement of this document. This will normally correspond to the Document Availability (11). However, where further distribution (beyond the audience specified in (11) is possible, a wider announcement audience may be selected.)  Unlimited			

13. **ABSTRACT** (A brief and factual summary of the document. It may also appear elsewhere in the body of the document itself. It is highly desirable that the abstract of classified documents be unclassified. Each paragraph of the abstract shall begin with an indication of the security classification of the information in the paragraph (unless the document itself is unclassified) represented as (S), (C), (R), or (U). It is not necessary to include here abstracts in both official languages unless the text is bilingual.)

The results of wearing superhydrophobic surfaces and its effect on roughness parameters, surface properties and wetting behaviour are described in this report. An abrasive wear device has been set up to allow consistency, reproducibility and precise control over the amount of wear desired. Based on the results obtained, relationships in the trends observed with the different roughness parameters and wetting behaviour have been established. In some cases the relationships are strong while in other cases, the relationships are weak and unable to capture the different transitions in wetting. It has also been determined that different roughness scales present on a surface wear differently and require separate attention. This knowledge is partly applied in the development of a versatile superhydrophobic coating that can be used on smooth and rough materials ranging from glass and aluminum, to polyester/nylon, cardboard and wood.

Le présent rapport contient la description de l'usure subie par des surfaces superhydrophobes et de ses effets sur les paramètres de rugosité, les propriétés de surface et le comportement au mouillage. On a mis en place un dispositif d'usure par abrasion qui permet d'assurer un contrôle précis, uniforme et reproductible du degré d'usure souhaité. Les résultats obtenus ont permis d'établir des relations à partir des tendances observées pour les différents paramètres de rugosité et le comportement au mouillage. Dans certains cas, les relations sont solides ( $R_{sk}$ ,  $S_{sk}$ ,  $r$ ), alors que dans d'autres, elles sont faibles ( $R_a$ ,  $R_q$ ,  $R_z$ ) et ne permettent pas d'extraire les diverses transitions qui surviennent au cours du mouillage. Les résultats ont aussi permis de déterminer que des zones de la surface caractérisées par diverses échelles de rugosité subissent une usure différente et nécessitent donc des mesures de protection distinctes. Ces connaissances peuvent être en partie utilisées pour mettre au point un revêtement superhydrophobe polyvalent pouvant être appliqué sur des matériaux lisses et rugueux, dans une gamme allant du verre et de l'aluminium au carton et au bois, en passant par des polymères comme les polyesters et les nylons.

14. **KEYWORDS, DESCRIPTORS or IDENTIFIERS** (Technically meaningful terms or short phrases that characterize a document and could be helpful in cataloguing the document. They should be selected so that no security classification is required. Identifiers, such as equipment model designation, trade name, military project code name, geographic location may also be included. If possible keywords should be selected from a published thesaurus, e.g. Thesaurus of Engineering and Scientific Terms (TEST) and that thesaurus identified. If it is not possible to select indexing terms which are Unclassified, the classification of each should be indicated as with the title.)

Roughness; Confocal Microscopy; Contact Angle; wettability; Superhydrophobic;

This page intentionally left blank.

## **Defence R&D Canada**

Canada's leader in defence  
and National Security  
Science and Technology

## **R & D pour la défense Canada**

Chef de file au Canada en matière  
de science et de technologie pour  
la défense et la sécurité nationale



[www.drdc-rddc.gc.ca](http://www.drdc-rddc.gc.ca)